

PB97171011



Testing of New Bridge Rail and Transition Designs

Volume XIV: Appendix M

Axial Tensile Strength of Thrie and W-Beam Terminal Connectors

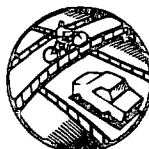
PUBLICATION NO. FHWA-RD-93-157

JUNE 1997



U.S. Department of Transportation
Federal Highway Administration

Research and Development
Turner-Fairbank Highway Research Center
6300 Georgetown Pike
McLean, VA 22101-2296




REPRODUCED BY: **NTIS**
U.S. Department of Commerce
National Technical Information Service
Springfield, Virginia 22161

FOREWORD

This report presents the results of a State Planning and Research (SP&R) pooled-fund study to develop safer bridge rail and transition designs. This pooled-fund study was sponsored by the Federal Highway Administration, 23 States, and the District of Columbia. A panel of representatives from those agencies selected the designs to be studied. Ten bridge rails and two transitions were designed and crash tested in accordance with the recommendations for the various Performance Levels in the *1989 AASHTO Guide Specifications for Bridge Railings*. Acceptable performance was demonstrated for all of the crash tested designs.

Detailed drawings are presented for documentation and to facilitate implementation.


A. George Ostensen, Director
Office of Safety and Traffic
Operations, Research and
Development

NOTICE

This document is disseminated under the sponsorship of the Department of Transportation in the interest of information exchange. The United States Government assumes no liability for its contents or use thereof. This report does not constitute a standard, specification, or regulation.

The United States Government does not endorse products or manufacturers. Trade and manufacturer's names appear in this report only because they are considered essential to the object of the document.

1. Report No. FHWA-RD-93-157		2. Government Accession No.		3. Recipient's Catalog No.	
4. Title and Subtitle TESTING OF NEW BRIDGE RAIL AND TRANSITION DESIGNS Volume XIV: Appendix M Axial Tensile Strength of Thrie and W-Beam Terminal Connectors				5. Report Date June 1997	
				6. Performing Organization Code	
7. Author(s) C. Eugene Buth, T. J. Hirsch, and Matt Henderson				8. Performing Organization Report No. Research Foundation 7069-Vol. XIV	
9. Performing Organization Name and Address Texas Transportation Institute The Texas A&M University System College Station, Texas 77843-3135				10. Work Unit No. NCP No. 3A5C0042	
				11. Contract or Grant No. DTFH61-86-C-00071	
12. Sponsoring Agency Name and Address Office of Safety & Traffic Operations R&D Federal Highway Administration 6300 Georgetown Pike McLean, Virginia 22101-2296				13. Type of Report and Period Covered Final Report August 1986 - September 1993	
				14. Sponsoring Agency Code	
15. Supplementary Notes Research performed in cooperation with DOT, FHWA Research Study Title: Pooled Funds Bridge Rail Study Contracting Officer's Technical Representative (COTR) - Charles F. McDevitt					
16. Abstract In some connections of w-beam and thrie-beam guardrail elements, it is necessary to bolt together three thicknesses of rail element. Such a connection can not be assembled without enlarging the standard round connection bolt holes. One solution to this problem is to use elongated holes with the long axis of the hole at an angle to the longitudinal axis of the rail element. A number of static load tests were performed to investigate the strength of terminal connectors with slanted elongated splice holes. This volume is the fourteenth in a series. The other volumes in the series are: Volume I: Technical Report; Volume II: Appendix A, Oregon Side Mounted Bridge Railing; Volume III: Appendix B, BR27D Bridge Railing; Volume IV: Appendix C, Illinois 2399-1 Bridge Railing; Volume V: Appendix D, 32-in (813-mm) Concrete Parapet Bridge Railing; Volume VI: Appendix E, 32-in (813-mm) New Jersey Safety Shape; Volume VII: Appendix F, 32-in (813-mm) F-Shape Bridge Railing; Volume VIII: Appendix G, BR27C Bridge Railing; Volume IX: Appendix H, Illinois Side Mount Bridge Rail; Volume X: Appendix I, 42-in (1.07-m) Concrete Parapet Bridge Railing; Volume XI: Appendix J, 42-in (1.07-m) F-Shape Bridge Railing; Volume XII: Appendix K, Oregon Transition; and Volume XIII: Appendix L, 32-in (813-mm) Thrie-Beam Transition.					
17. Key Words Guardrail, Bridge Railing, W-beam, Thrie-Beam, Terminal Connector, Load Tests, Ultimate Strength			18. Distribution Statement No restrictions. This document is available to the public through the National Technical Information Service 5285 Port Royal Road Springfield, Virginia 22161		
19. Security Classif. (of this report) Unclassified		20. Security Classif. (of this page) Unclassified		21. No. of Pages 55	22. Price

SI* (MODERN METRIC) CONVERSION FACTORS

APPROXIMATE CONVERSIONS TO SI UNITS

APPROXIMATE CONVERSIONS FROM SI UNITS

Symbol	When You Know	Multiply By	To Find	Symbol	Symbol	When You Know	Multiply By	To Find	Symbol
LENGTH					LENGTH				
in	inches	25.4	millimeters	mm	mm	millimeters	0.039	inches	in
ft	feet	0.305	meters	m	m	meters	3.28	feet	ft
yd	yards	0.914	meters	m	m	meters	1.09	yards	yd
mi	miles	1.61	kilometers	km	km	kilometers	0.621	miles	mi
AREA					AREA				
in ²	square inches	645.2	square millimeters	mm ²	mm ²	square millimeters	0.0016	square inches	in ²
ft ²	square feet	0.093	square meters	m ²	m ²	square meters	10.764	square feet	ft ²
yd ²	square yards	0.836	square meters	m ²	m ²	square meters	1.195	square yards	yd ²
ac	acres	0.405	hectares	ha	ha	hectares	2.47	acres	ac
mi ²	square miles	2.59	square kilometers	km ²	km ²	square kilometers	0.386	square miles	mi ²
VOLUME					VOLUME				
fl oz	fluid ounces	29.57	milliliters	mL	mL	milliliters	0.034	fluid ounces	fl oz
gal	gallons	3.785	liters	L	L	liters	0.264	gallons	gal
ft ³	cubic feet	0.028	cubic meters	m ³	m ³	cubic meters	35.71	cubic feet	ft ³
yd ³	cubic yards	0.765	cubic meters	m ³	m ³	cubic meters	1.307	cubic yards	yd ³
NOTE: Volumes greater than 1000 l shall be shown in m ³ .									
MASS					MASS				
oz	ounces	28.35	grams	g	g	grams	0.035	ounces	oz
lb	pounds	0.454	kilograms	kg	kg	kilograms	2.202	pounds	lb
T	short tons (2000 lb)	0.907	megagrams (or "metric ton")	Mg (or "t")	Mg (or "t")	megagrams (or "metric ton")	1.103	short tons (2000 lb)	T
TEMPERATURE (exact)					TEMPERATURE (exact)				
°F	Fahrenheit temperature	5(F-32)/9 or (F-32)/1.8	Celcius temperature	°C	°C	Celcius temperature	1.8C + 32	Fahrenheit temperature	°F
ILLUMINATION					ILLUMINATION				
fc	foot-candles	10.76	lux	lx	lx	lux	0.0929	foot-candles	fc
fl	foot-Lamberts	3.426	candela/m ²	cd/m ²	cd/m ²	candela/m ²	0.2919	foot-Lamberts	fl
FORCE and PRESSURE or STRESS					FORCE and PRESSURE or STRESS				
lbf	poundforce	4.45	newtons	N	N	newtons	0.225	poundforce	lbf
lbf/in ²	poundforce per square inch	6.89	kilopascals	kPa	kPa	kilopascals	0.145	poundforce per square inch	lbf/in ²

* SI is the symbol for the International System of Units. Appropriate rounding should be made to comply with Section 4 of ASTM E380.

TABLE OF CONTENTS

<u>Chapter</u>	<u>Page</u>
1. INTRODUCTION	1
2. TEST DESCRIPTION	5
3. TEST RESULTS	11
4. CONCLUSIONS	35

LIST OF FIGURES

<u>Figure No.</u>	<u>Page</u>
1. Standard thrie-beam.	2
2. Standard W-beam	3
3. Steel plate attachment for flat section of terminal connector.	6
4. Steel plate attachment for test piece.	7
5. Views of SAE 4140 high strength steel yoke.	8
6. Terminal connector test assembly for a thrie-beam.	9
7. Terminal connector test specimens.	12
8. Connector and test piece prior to test, sample one.	14
9. View of flat section prior to test, sample one.	14
10. Exterior damage to flat section, sample one.	16
11. Interior damage to flat section, sample one.	16
12. Connector and test piece prior to test, sample two.	17
13. Exterior damage to flat section, sample two.	17
14. Interior damage to flat section, sample two.	17
15. Connector and test piece prior to test, sample three.	18
16. Exterior view of damaged connector, sample three.	18
17. Connector and test piece prior to test, sample four.	19
18. Exterior damage to flat section, sample four.	19
19. Connector and test piece before test, sample five.	20
20. Interior damage to flat section, sample five.	20
21. Exterior damage to flat section, sample five.	22
22. Full view of exterior damage, sample five.	22
23. Exterior damage to flat section, sample six.	23
24. Interior damage to flat section, sample six.	23
25. Full view of damaged connector, sample six.	24
26. Damage at splice connection, sample six.	24
27. Terminal connector and test piece after test, sample eight.	25
28. Exterior damage to flat section, sample eight.	25
29. Local buckling at edge of connector, sample eight.	25
30. Exterior damage to flat section, sample nine.	26
31. Interior damage to flat section, sample nine.	26
32. Terminal connector prior to testing.	27
33. Exterior damage at flat section, sample ten.	27
34. Interior damage of flat section, sample ten.	27
35. Interior view of terminal connector after test, sample eleven.	28
36. Exterior damage to flat section, sample eleven.	28
37. Exterior damage to flat section, sample twelve.	30
38. Interior damage to flat section, sample twelve.	30
39. Damage at splice end, sample twelve.	30
40. Damage at flat section, sample thirteen.	31

LIST OF FIGURES (Continued)

<u>Figure No.</u>	<u>Page</u>
41. Damage at flat section, sample fourteen.	31
42. Damage at flat section, sample fifteen.	32
43. Damage at splice end, sample thirteen.	32
44. Damage at splice end, sample fourteen.	33
45. Damage at splice end, sample fifteen.	33
46. Local buckling of terminal connector, sample thirteen.	34
47. Local buckling of terminal connector, sample fourteen.	34
48. Local buckling of terminal connector, sample fifteen.	34
49. Load vs. displacement graph, sample one	36
50. Load vs. displacement graph, sample two.	37
51. Load vs. displacement graph, sample three.	38
52. Load vs. displacement graph, sample four.	39
53. Load vs. displacement graph, sample five.	40
54. Load vs. displacement graph, sample six.	41
55. Load vs. displacement graph, sample eight.	42
56. Load vs. displacement graph, sample nine.	43
57. Load vs. displacement graph, sample ten.	44
58. Load vs. displacement graph, sample eleven.	45
59. Load vs. displacement graph, sample twelve.	46
60. Load vs. displacement graph, sample thirteen.	47
61. Load vs. displacement graph, sample fourteen.	48
62. Load vs. displacement graph, sample fifteen	49

LIST OF TABLES

<u>Table No.</u>	<u>Page</u>
1. Ultimate loads and properties of w-beam and thrie beam terminal connectors.	15

CHAPTER 1. INTRODUCTION

The standard ARTBA (American Road and Transportation Builders Association) terminal connector is a section formed in the shape of a thrie- or w-beam guardrail at one end and tapered to a flat section at the other end. The flat portion of the terminal connector is suitable for attaching to a bridge abutment or parapet wall, while the rail end is spliced to the guardrail.

Standard ARTBA thrie-beam terminal connectors have five 1-in (25.4-mm) diameter holes located in the flat portion, and the w-beams have four 1-in (25.4-mm) diameter holes. The rail end of the thrie-beam terminal connector provides fourteen (twelve splice and two post) elongated bolt slots that are parallel to the longitudinal axis; whereas the w-beam terminal connector provides nine (eight splice and one post) elongated slots at the splice end (figures 1 and 2). Typical thrie-beam terminal connectors are fabricated from two w-beam terminal connectors with a welded seam along longitudinal axis. Sample five was the only thrie-beam terminal connector without a welded seam in this experiment.

Nested guardrail elements are sometimes used to increase the stiffness near the parapet wall of the bridge. It is impossible to connect nested guardrail elements to a standard ARTBA terminal connector (straight slots) without damaging the elements. To circumvent this problem, angled slots (angled from the longitudinal axis) were punched in the rail end of the terminal connector thus enabling the splice bolts to pass through all three elements; however, using angled slots may reduce the axial tensile load capacity of the terminal connector to an unacceptable degree. To help answer this question of reduction in strength, eleven samples were tested in axial tension at the contractor's structures laboratory. Descriptions of the tests and their results are presented in the following pages.

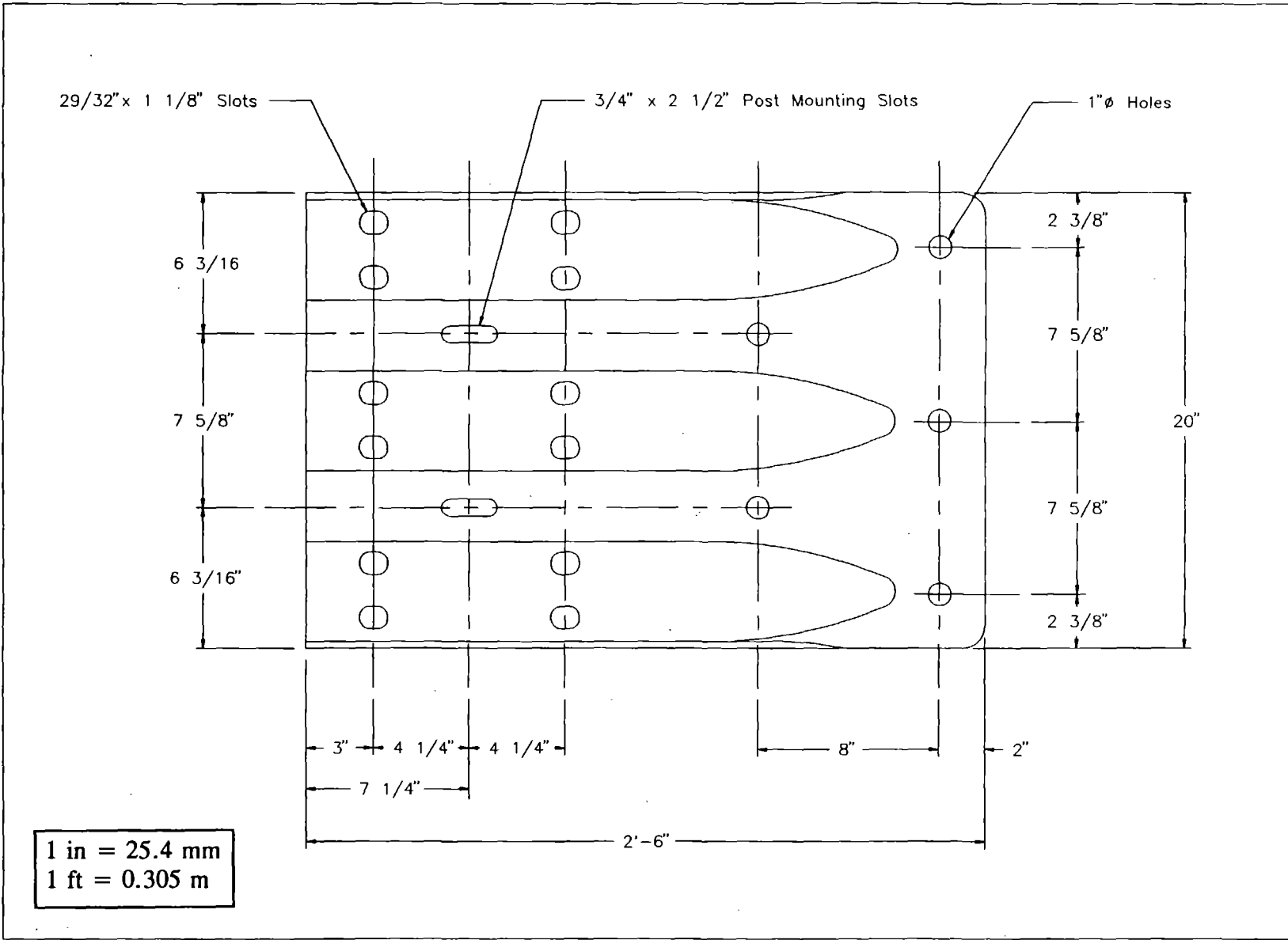
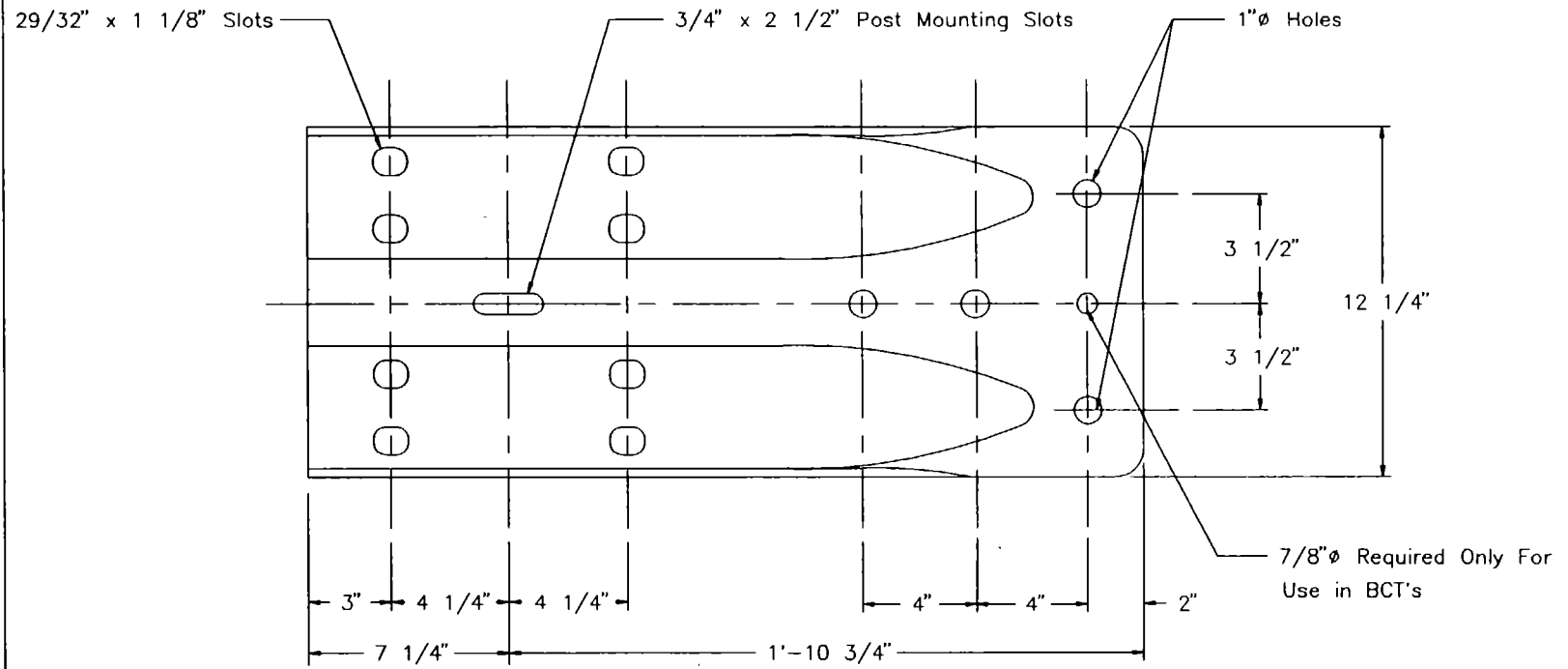


Figure 1. Standard thrie-beam.



1 in = 25.4 mm
1 ft = 0.305 m

Figure 2. Standard W-beam.

CHAPTER 2. TEST DESCRIPTION

The loading device used to apply axial tension to each sample was the MTS (Material Testing System) 2000 which has a tensile or compression loading capacity of 500 kips (2 224 kN). The machine is equipped with female threaded couplings on the stationary (load) and transient (ram) ends. In order to utilize the MTS 2000, an adapter consisting of two male threaded yokes and two steel plates was constructed.

The plates were fabricated from ASTM A36 steel. One plate had predrilled holes to match the holes on the flat portion of the terminal connectors, while the other plate had predrilled holes for matching the holes in the test pieces (figures 3 and 4). Additionally, each plate had a 3-in (76.2-mm) diameter pin hole located near the throat of the plate.

The yokes were machined from 6-in (152.4-mm) diameter SAE 4140 high strength steel (figure 5). One end of the yoke was threaded to match the 4-in (102-mm) diameter female couplings of the MTS 2000. A 1-in (25.4-mm) groove was machined in the other end of the yoke spanning the diameter, and a 3-in (76.2-mm) diameter pin hole was drilled perpendicular to the groove through the diameter of the yoke.

The pins for the "adapter" assembly were fabricated from 3-in (76.2-mm) diameter 17-4'PH H900 high strength stainless steel. The pins were 6-in (152-mm) long and spanned the diameter of the yoke.

Each threaded male end of the yoke was placed into the female end of the MTS 2000. The steel plates were then placed in the groove of the yokes, aligning the pin holes. The pin was placed through both plate and yoke, allowing rotation about the Y-Y axis of the cross section of the terminal connector.

The terminal connector was bolted to the stationary (upper) plate at its flat section. The test piece, a 36-in (914-mm) long segment of guard rail, was bolted to the transient (lower) plate (see figure 6). SAE grade 8 high strength bolts, flat and lock washers, and nuts were used for all test samples at these connections. The test piece and terminal connector for all samples were spliced together using ASTM A307 button-head splice bolts and A563 flat washers and nuts. All high strength bolts were torqued to 473 ft-lb (632 N-m), and all mild steel bolts were torqued to 70 ft-lb (95 N-m). Each sample was loaded at the rate of 0.1 in/min (2.5 mm/min) and tested for ultimate strength under static, axial tension loading. A GS-2000 Servo Controller/Data Acquisition System was used for recording the load and ram head displacement data every second. An initial vertical position of the ram head was input into the system. Ram head displacement data was relative to that position, and many of the graphs in the results reflect this relative positioning. Additionally, each sample was subjected to a preloaded condition (maximum of 6 kips (27 kN)) to remove slack in the system.

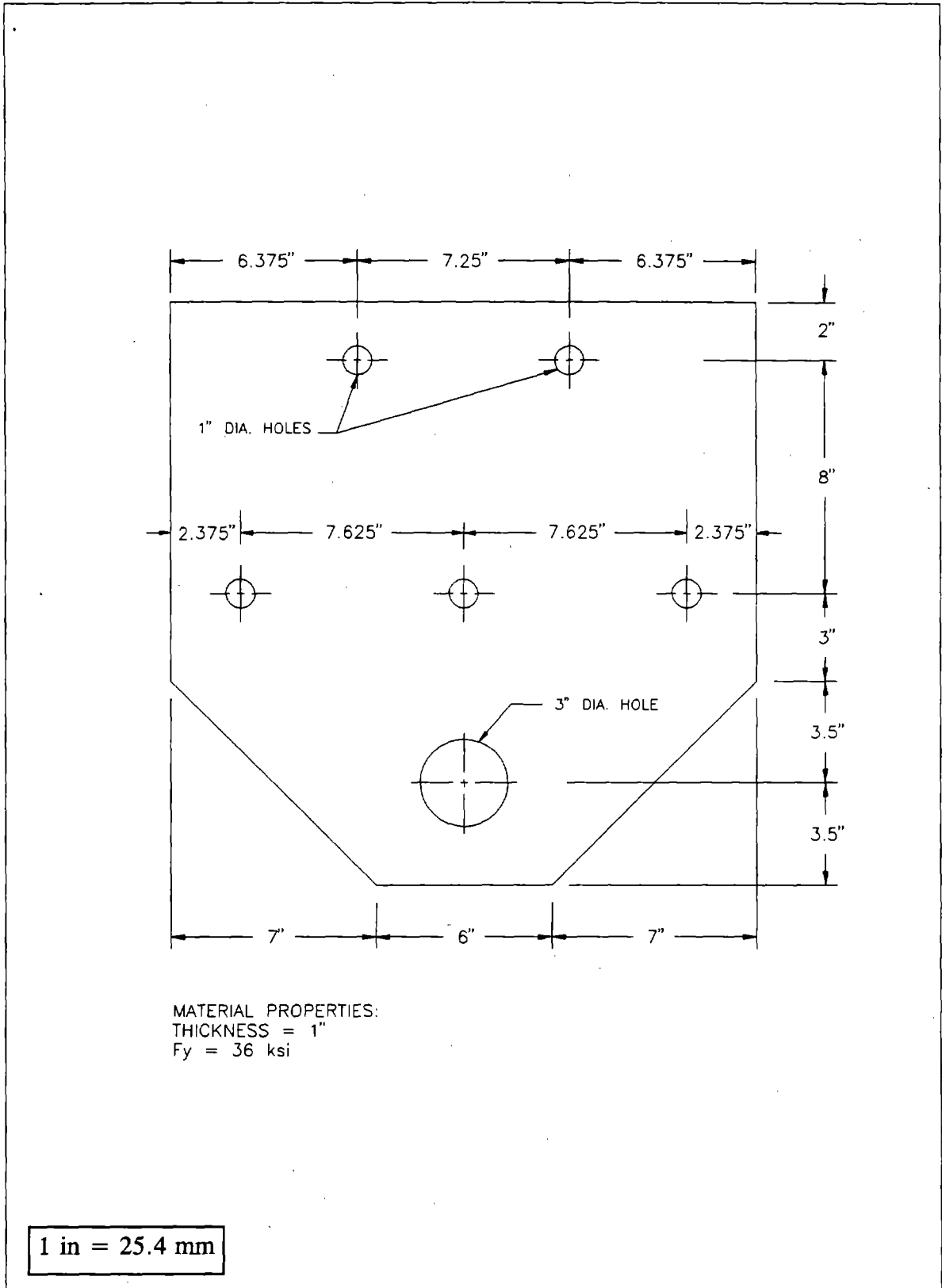


Figure 3. Steel plate attachment for flat section of terminal connector.

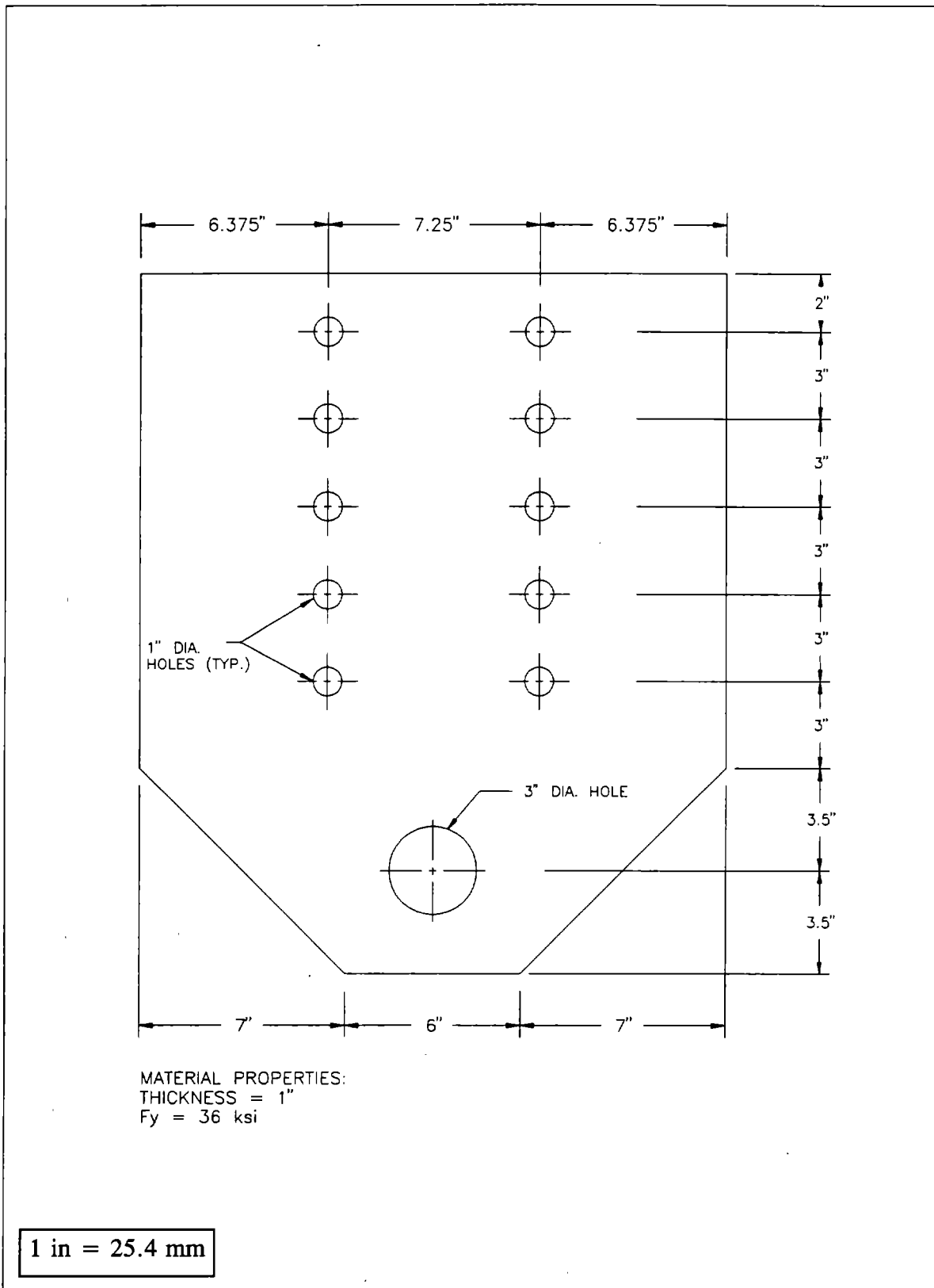


Figure 4. Steel plate attachment for test piece.

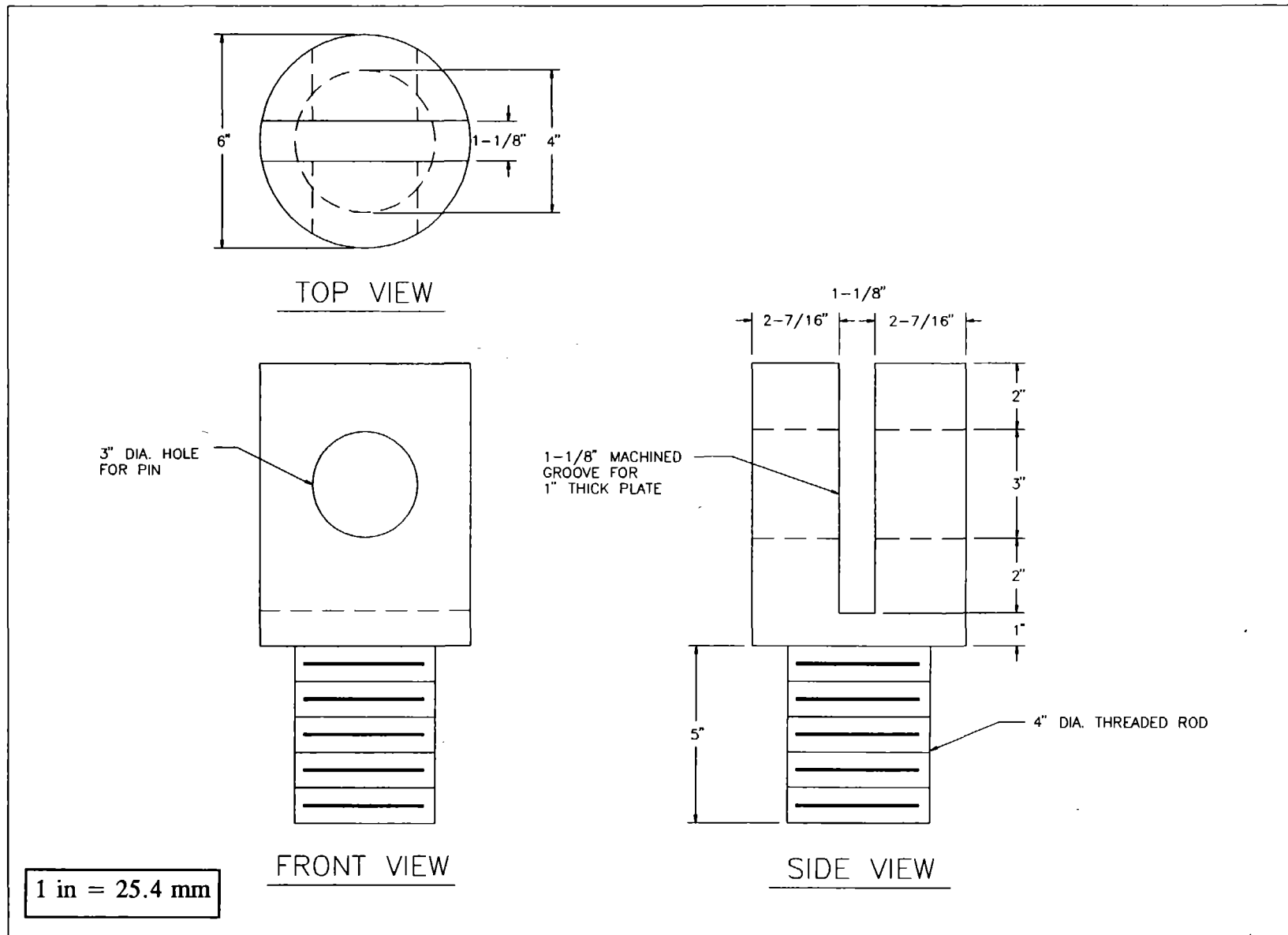


Figure 5. Views of SAE 4140 high strength steel yoke.

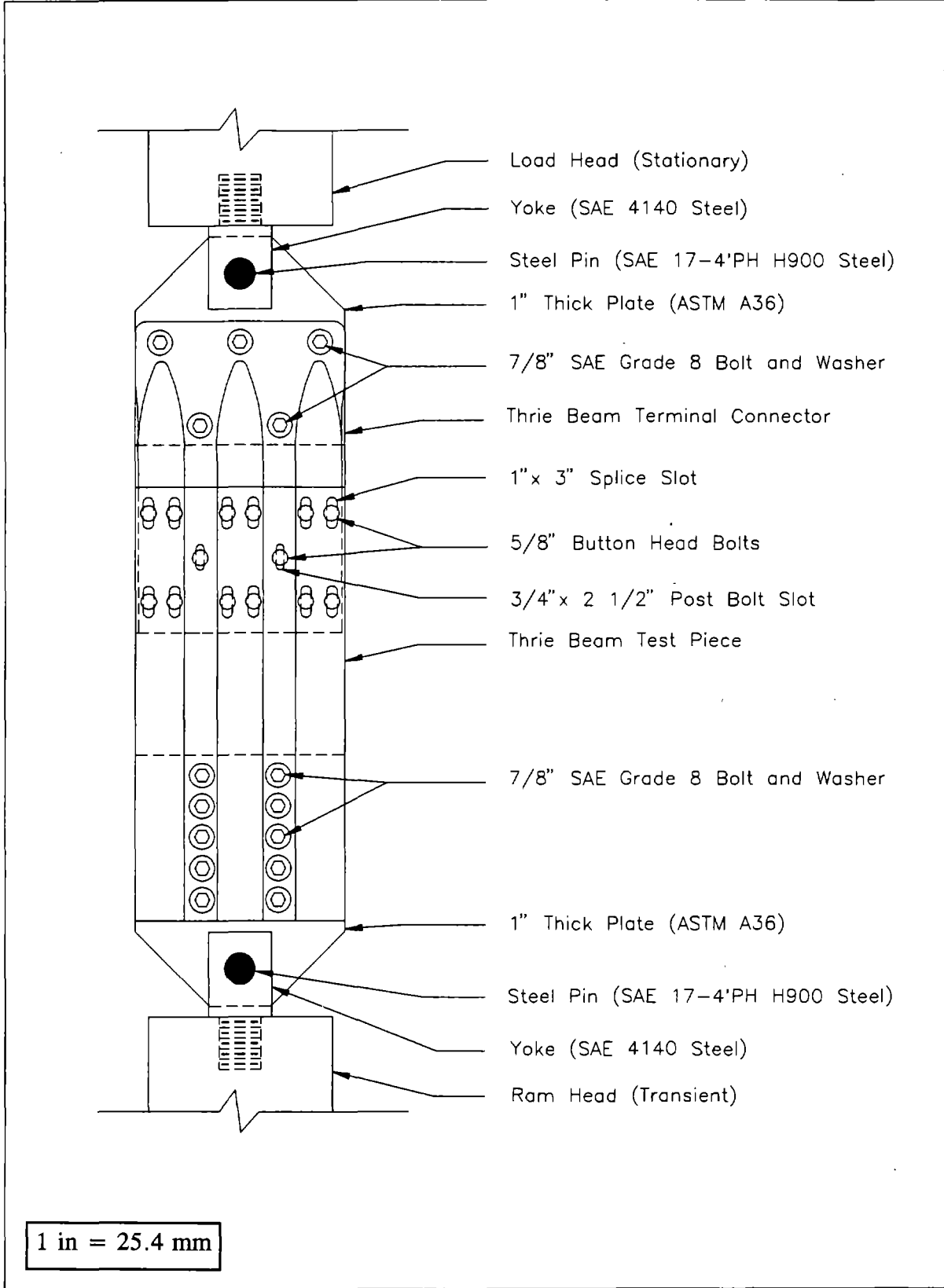


Figure 6. Terminal connector test assembly for a thrie-beam.

CHAPTER 3. TEST RESULTS

The first sample tested was a 10-gauge thrie-beam terminal connector fabricated by manufacturer #1 (figure 7). The flat portion of the terminal connector had five 1-in (25.4-mm) diameter bolt holes, and the rail end had twelve straight, elongated slots and two post mounting slots. Five 7/8-in (22.2-mm) diameter bolts were used in the flat section of the terminal connector, and fourteen 5/8-in (15.9-mm) diameter button-head bolts were used at the splice end (figures 8 and 9).

The sample failed in bearing of the 7/8-in (22.2-mm) diameter bolts onto the flat section of the terminal connector at 95.9 kips (426.6 kN) (table 1). Most of the deformation in the form of plastic flow occurred at the top row of bolt holes in the flat portion of the terminal connector (figures 10 and 11). There was relatively little or no deformation around the splice bolt slots.

Samples two, three, and four were 12-gauge thrie-beam terminal connectors fabricated by manufacturer #2 (figure 7). The flat portion of each terminal connector had seven 1-in (25.4-mm) diameter holes and two 7/8-in (22.2-mm) diameter holes. The splice end had 12 angled splice slots and two post mounting slots. Seven 7/8-in (22.2-mm) diameter bolts and two 3/4-in (19.1-mm) diameter bolts were used in the flat section of the terminal connector, and fourteen 5/8-in (16-mm) diameter button-head bolts were used at the splice end (figures 12, 13, and 14).

Failure of sample two was in bearing of the 7/8-in (22.2-mm) diameter bolts onto the flat section. Further displacement caused tearing normal to the load at the outside two holes of the top row (figures 15 and 16). As in sample one, there was relatively little or no deformation at the splice bolt connection. The ultimate load capacity of this terminal connector was 132.6 kips (589.8 kN) (table 1). Note that sample two was fabricated from 12-gauge steel, yet its load capacity was approximately 40 kips (178 kN) greater than sample one fabricated from 10-gauge steel. The load capacity differential can be attributed to the difference in the number of bolts used in the two samples.

Samples three and four were tested in precisely the same manner as sample two with similar results. Ultimate loads were 126.8 kips (564.0 kN) and 133.7 kips (594.7 kN), respectively (table 1). Failure for both was in bearing of the 7/8-in (22.2-mm) diameter bolts onto the flat portion of the terminal connector. Further displacement caused tearing at the outside two holes of the top row of the flat section. Sample three exhibited some deformation at the splice bolt connection, while sample four had relatively little or none (figures 17 and 18).

Sample five was a 10-gauge thrie-beam terminal connector fabricated by manufacturer #3 (figure 7). It had five 1-in (25.4-mm) diameter bolt holes at the flat portion of the terminal connector and longitudinally straight, short slots at the splice end. The assembly of bolts was identical to sample one (figure 19). The sample failed in bearing of the 7/8-in (22.2-mm) diameter bolts onto the flat end at 116.7 kips (519.1 kN) (table 1). Most of the

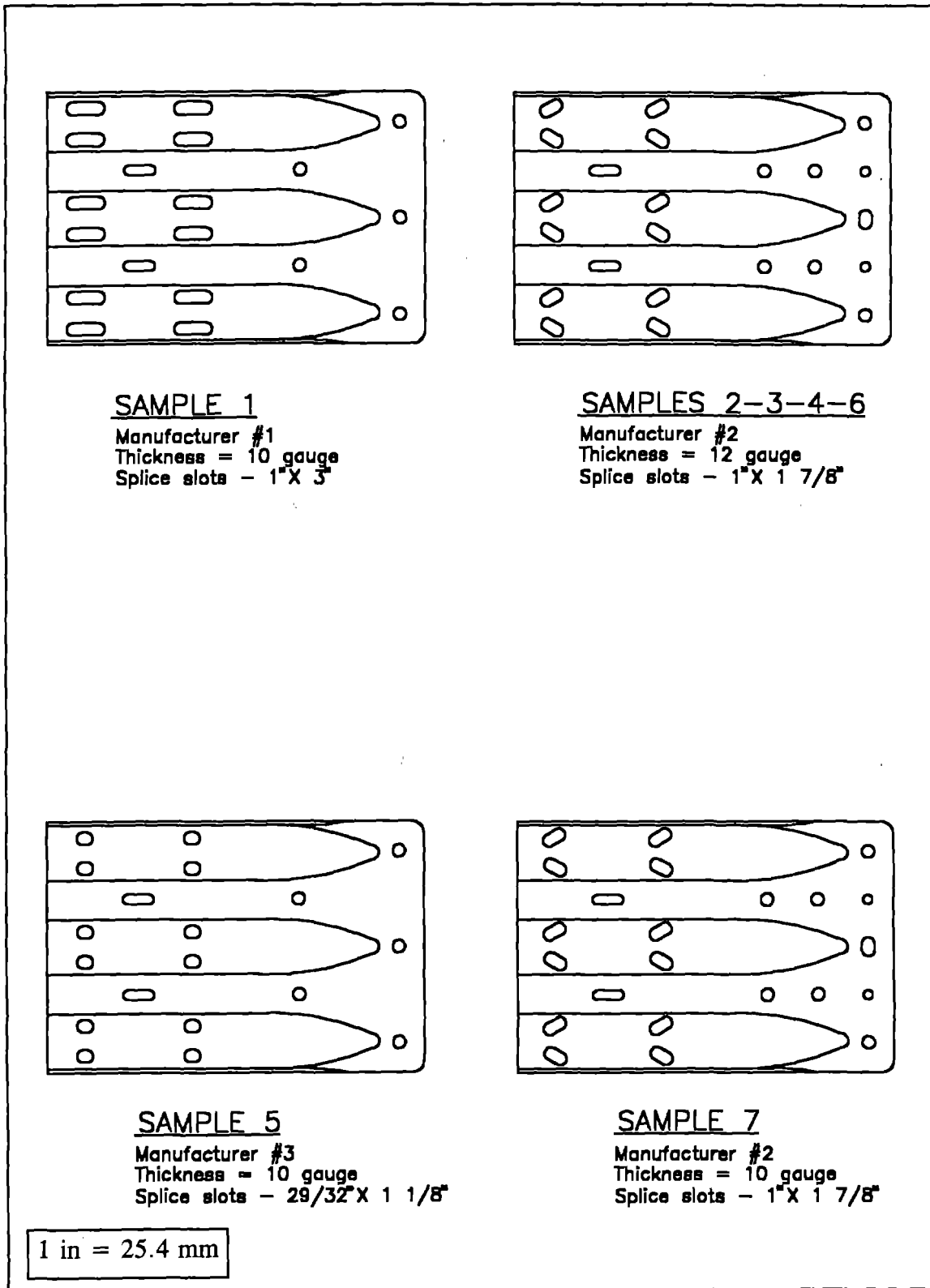
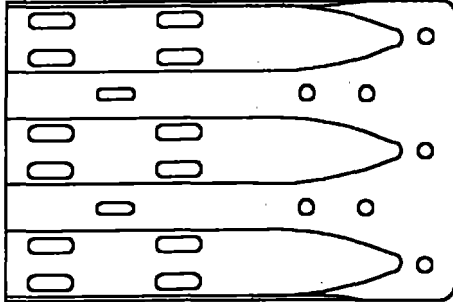
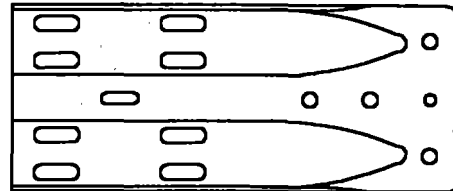


Figure 7. Terminal connector test specimens.



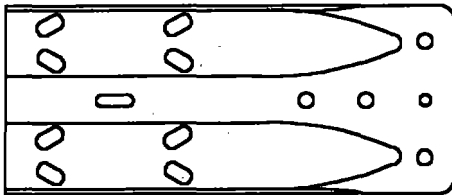
SAMPLES 8-9

Manufacturer #1
 Thickness = 10 gauge
 Splice slots - 1" X 3"



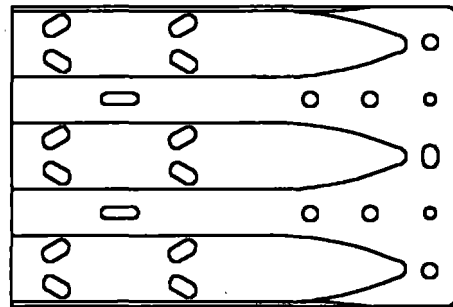
SAMPLE 12

Manufacturer #2
 Thickness = 12 gauge
 Splice slots - 1" X 3"



SAMPLES 10-11

Manufacturer #2
 Thickness = 12 gauge
 Splice slots - 1" X 1 7/8"



SAMPLES 13-14-15

Manufacturer #2
 Thickness = 10 gauge
 Splice slots - 1" X 1 7/8"

1 in = 25.4 mm

Figure 7. Terminal connector test specimens (continued).

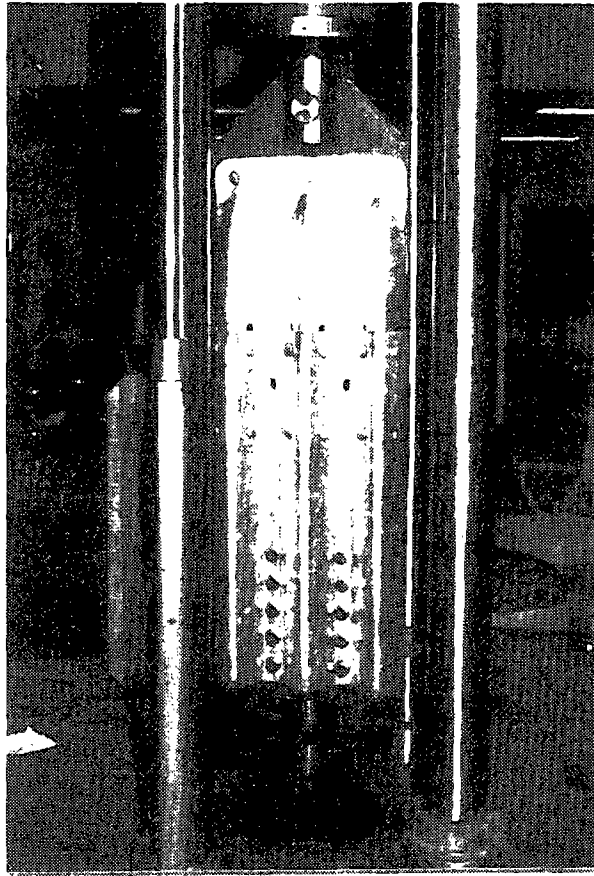


Figure 8. Connector and test piece prior to test, sample one.

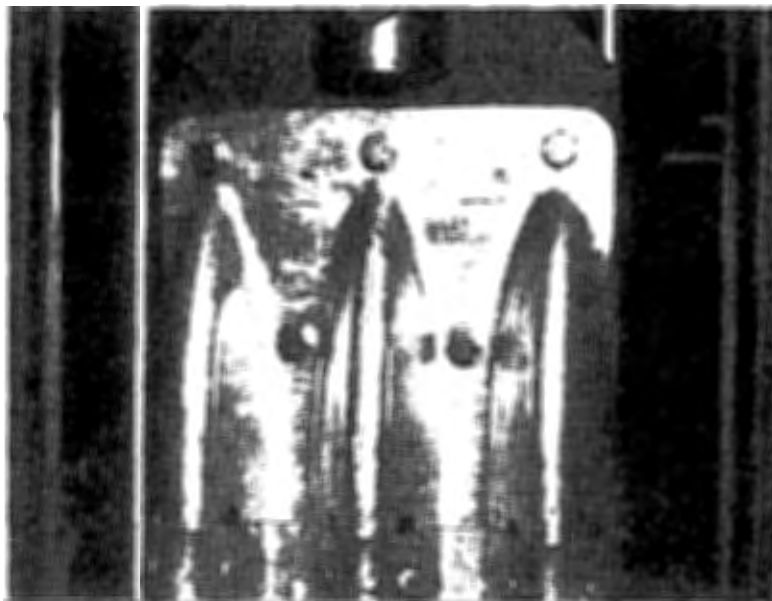


Figure 9. View of flat section prior to test, sample one.

Table 1. Ultimate loads and properties of W-beam and thrie-beam terminal connectors.

SAMPLE NO.	MANUFACTURER	MODEL	HOLE PATTERN	THICKNESS	NO. HOLES	ULTIMATE LOAD
1	NUMBER ONE	THRIE-BEAM	ST. LONG SLOTS	10 GAUGE	5 ¹	95.9 KIPS (426.6 kN)
2	NUMBER TWO	THRIE-BEAM	ANGLED SLOTS	12 GAUGE	9 ²	132.6 KIPS (589.8 kN)
3	NUMBER TWO	THRIE-BEAM	ANGLED SLOTS	12 GAUGE	9 ²	126.9 KIPS (564.5 kN)
4	NUMBER TWO	THRIE-BEAM	ANGLED SLOTS	12 GAUGE	9 ²	133.7 KIPS (594.7 kN)
5	NUMBER THREE	THRIE-BEAM	ST. SHORT SLOTS	10 GAUGE	5 ¹	116.7 KIPS (519.1 kN)
6	NUMBER TWO	THRIE-BEAM	ANGLED SLOTS	12 GAUGE	9 ¹	83.3 KIPS (370.5 kN)
7	NUMBER TWO	THRIE-BEAM	ANGLED SLOTS	10 GAUGE	9 ¹	- ⁴
8	NUMBER ONE	THRIE-BEAM	ST. LONG SLOTS	10 GAUGE	7 ¹	93.8 KIPS (417.2 kN)
9	NUMBER ONE	THRIE-BEAM	ST. LONG SLOTS	10 GAUGE	7 ¹	87.7 KIPS (390.1 kN)
10	NUMBER TWO	W-BEAM	ANGLED SLOTS	12 GAUGE	4 ³	65.9 KIPS (293.1 kN)
11	NUMBER TWO	W-BEAM	ANGLED SLOTS	12 GAUGE	4 ³	66.4 KIPS (295.4 kN)
12	NUMBER TWO	W-BEAM	ST. LONG SLOTS	12 GAUGE	4 ³	71.1 KIPS (316.3 kN)
13	NUMBER TWO	THRIE-BEAM	ANGLED SLOTS	10 GAUGE	9 ¹	102.4 KIPS (455.5 kN)
14	NUMBER TWO	THRIE-BEAM	ANGLED SLOTS	10 GAUGE	9 ¹	99.3 KIPS (441.7 kN)
15	NUMBER TWO	THRIE-BEAM	ANGLED SLOTS	10 GAUGE	9 ¹	101.8 KIPS (452.8 kN)

NOTES:

1. Terminal connectors tested with 5-SAE Grade 8, 7/8-in (22-mm) bolts at the flat section.
2. Terminal connectors tested with 7-SAE Grade 8, 7/8-in (22-mm) bolts and 2-SAE Grade 8, 3/4-in (19-mm) bolts at the flat section.
3. Terminal connectors tested with 4-SAE Grade 8, 7/8-in (22-mm) bolts at the flat section.
4. Sample 7 was used in crash test 7069-29.

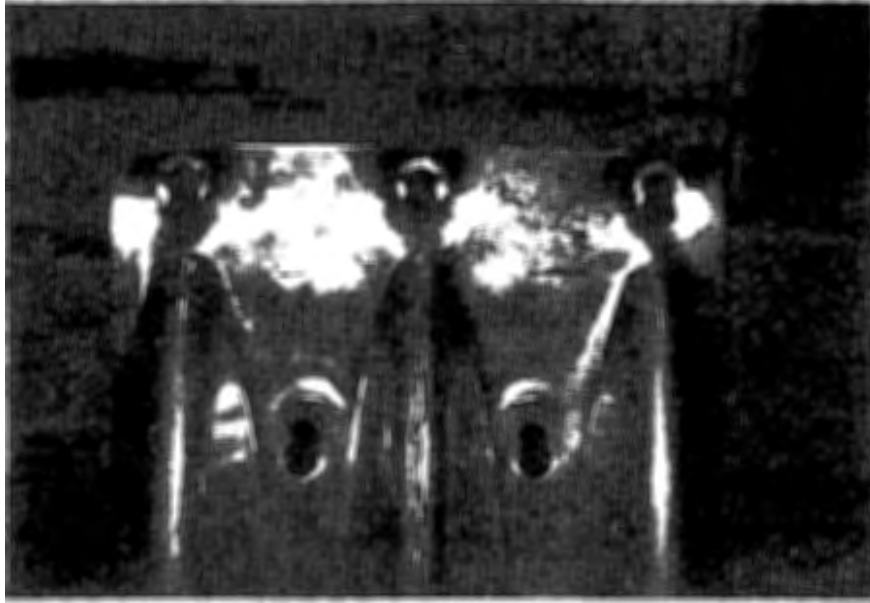


Figure 10. Exterior damage to flat section, sample one.

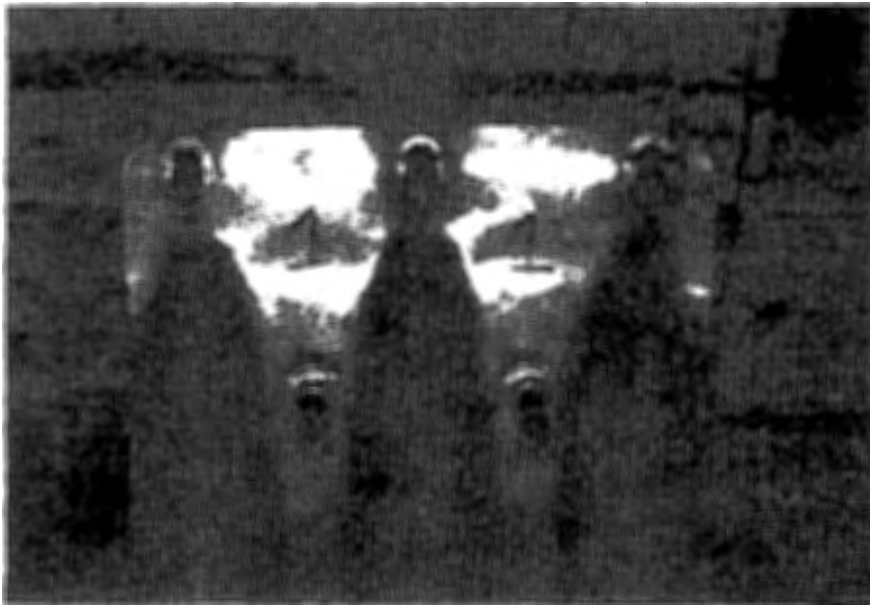


Figure 11. Interior damage to flat section, sample one.

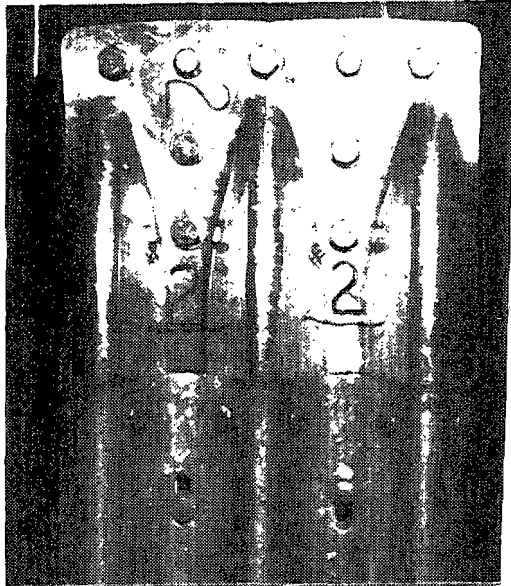


Figure 12. Connector and test piece prior to test, sample two.

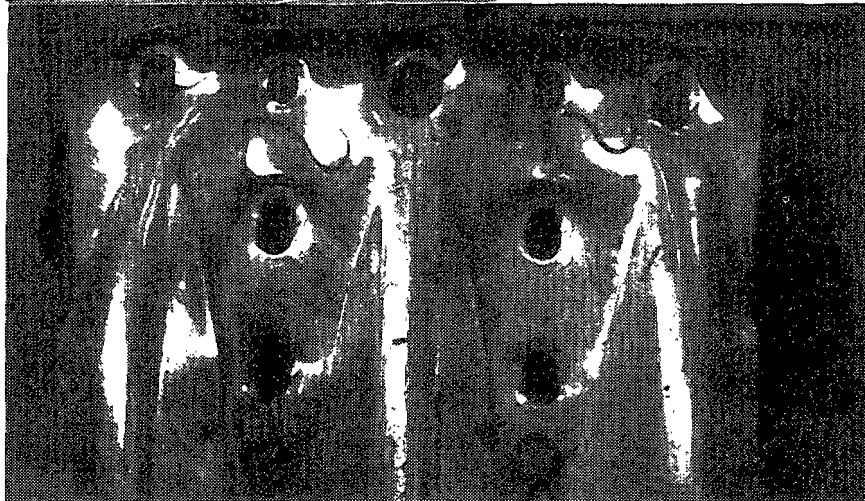


Figure 13. Exterior damage to flat section, sample two.

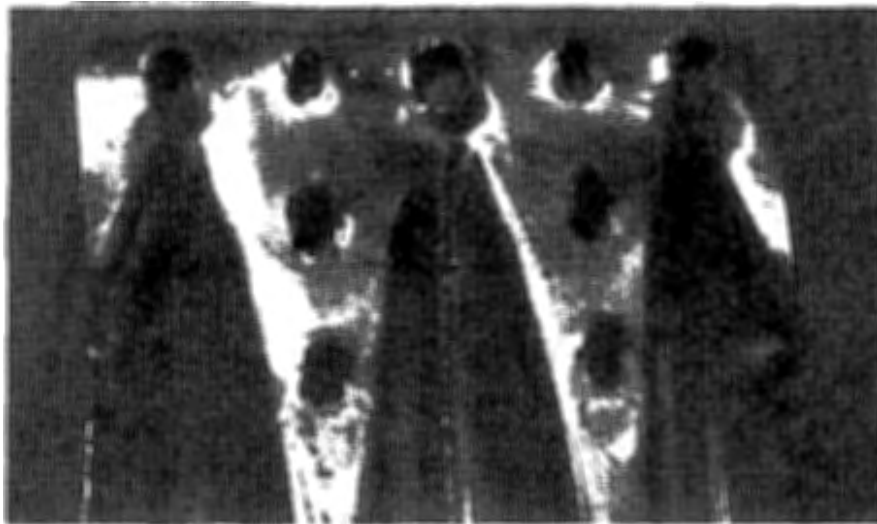


Figure 14. Interior damage to flat section, sample two.

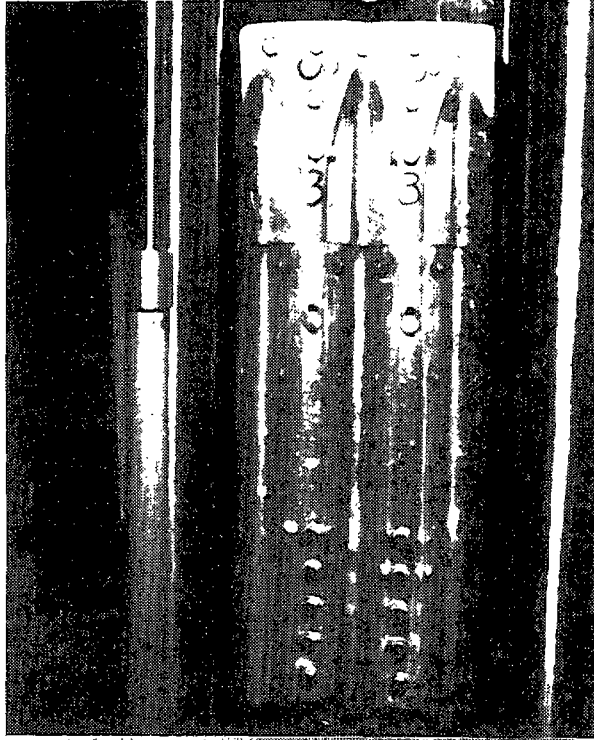


Figure 15. Connector and test piece prior to test, sample three.



Figure 16. Exterior view of damaged connector, sample three.

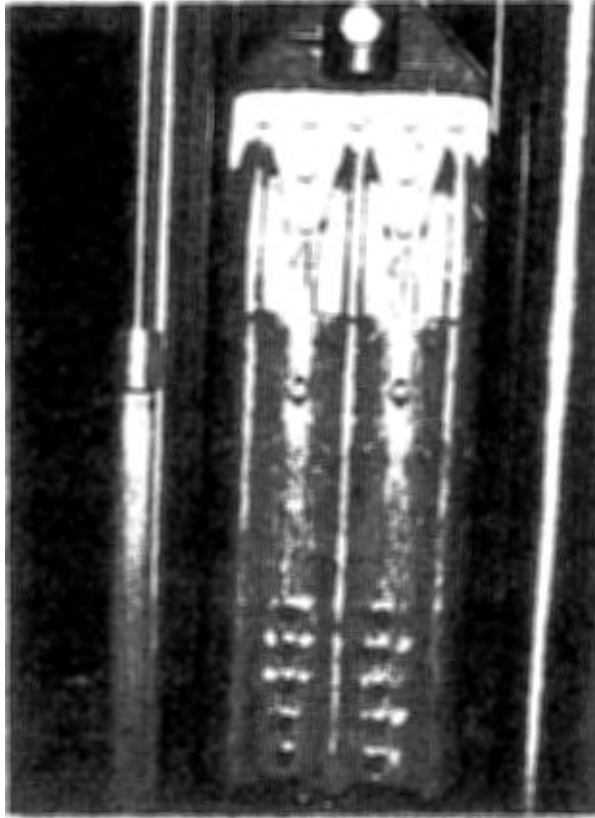


Figure 17. Connector and test piece prior to test, sample four.

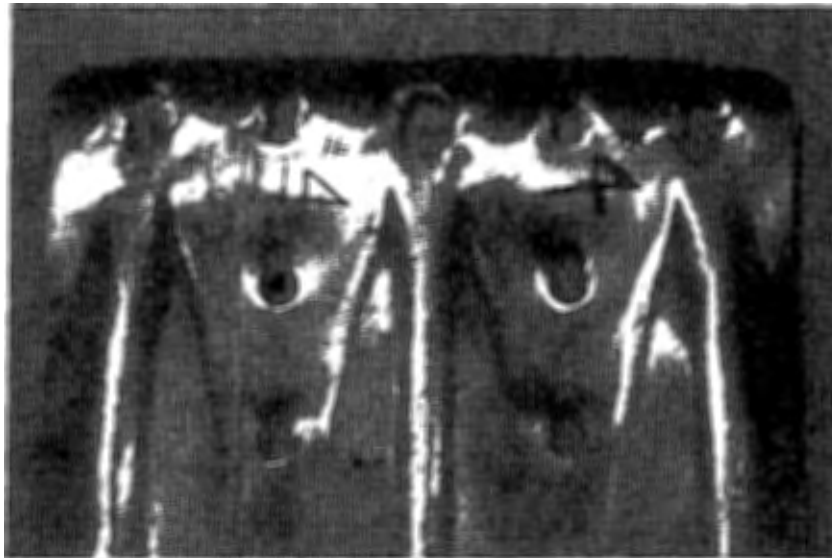


Figure 18. Exterior damage to flat section, sample four.



Figure 19. Connector and test piece before test, sample five.



Figure 20. Interior damage to flat section, sample five.

structural damage occurred at the top three bolt holes. Bearing of the bolts onto the connector followed by tearing normal to the direction of the load accounted for most of damage prior to the ultimate load capacity of the connector. Deformation at the splice bolt connection was once again limited (figures 20, 21, and 22).

Sample six was a 12-gauge thrie-beam terminal connector fabricated by manufacturer #2. Its hole and slot patterns were identical to samples two, three, and four (figure 7); however, this sample was tested with only five 7/8-in (22.2-mm) diameter bolts in the flat section. Failure was in bearing at 83.3 kips (370.5 kN) (table 1) and occurred at the 1-in (25.4-mm) diameter holes in the flat portion of the plate. Most of the deformation was plastic flow; however, some tearing occurred at the uppermost right hand bolt hole of the connector (figures 23 and 24). Little or no deformation was observed at the splice bolt connection (figures 25 and 26).

Samples eight and nine were 10-gauge thrie beam-terminal connectors fabricated by manufacturer #1 (figure 7). The flat sections consisted of seven 1-in (25.4-mm) diameter bolt holes, but only five 7/8-in (22.2-mm) diameter bolts were used in each of the samples (figure 27). The splice ends maintained longitudinally straight elongated slots.

Sample eight failed in bearing at 93.8 kips (417.2 kN) (table 1). There was considerable plastic flow at all bolt holes in the flat section, and the voids created by the bolts were much straighter and smoother than in previous tests. After further displacement, there was tearing normal to the direction of loading at the top row of 1-in (25.4-mm) diameter bolt holes in the flat section (figures 28 and 29).

Sample nine failed very similarly to sample eight at 87.7 kips (390.1 kN) (table 1). There was plastic flow at all bolt holes in the flat section of the terminal connector. The top row of 1-in (25.4-mm) bolt holes in the flat section showed extensive plastic deformation followed by tearing at the corners. There was no significant damage at the splice bolt connection (figures 30 and 31).

Samples ten and eleven were 12-gauge, w-beam terminal connectors fabricated by manufacturer #2. Each sample had four 1-in (25.4-mm) bolt holes in the flat section (figure 32). There were eight angled slots with one elongated post mounting slot at the splice end (figure 7). Each sample was tested with four 7/8-in (22.2-mm) diameter high strength bolts in the flat section and nine 5/8-in (16-mm) diameter button-head bolts at the splice end of the terminal connector. Both samples failed in bearing of the 7/8-in (22.2-mm) diameter bolts onto the flat section. The area between the top row of 7/8-in (22.2-mm) diameter bolts and the column of 7/8-in (22.2-mm) bolts buckled from differential deformation for both samples. The region near the top row of bolt holes, for instance, exhibited considerably more deformation than the region near the column of bolts (figures 33, 34, and 35). Unlike previous tests, sample ten exhibited no tearing at any of the bolt holes in the flat section of the terminal connector. There was, however, some deformation on all eight splice holes. Sample eleven had tearing in the upper row of bolt holes. The tearing was angled from the longitudinal axis, unlike most of the other samples in which the tearing was normal to the

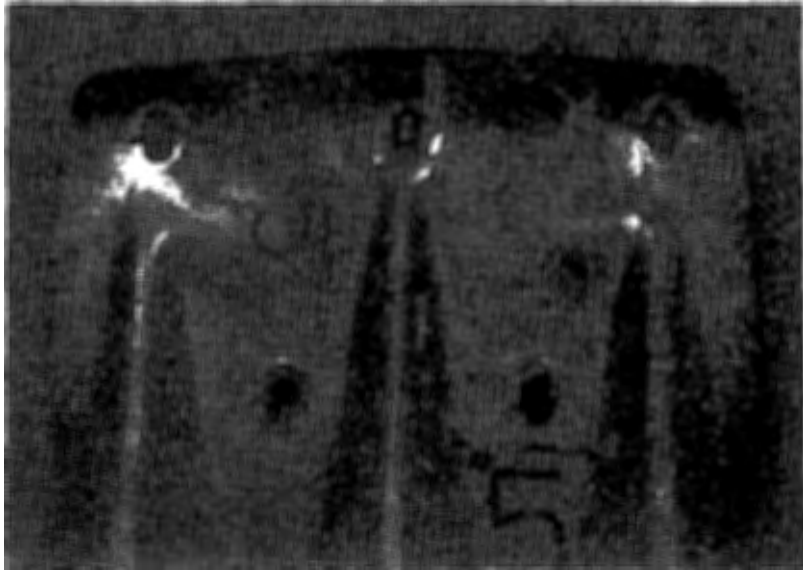


Figure 21. Exterior damage to flat section, sample five.

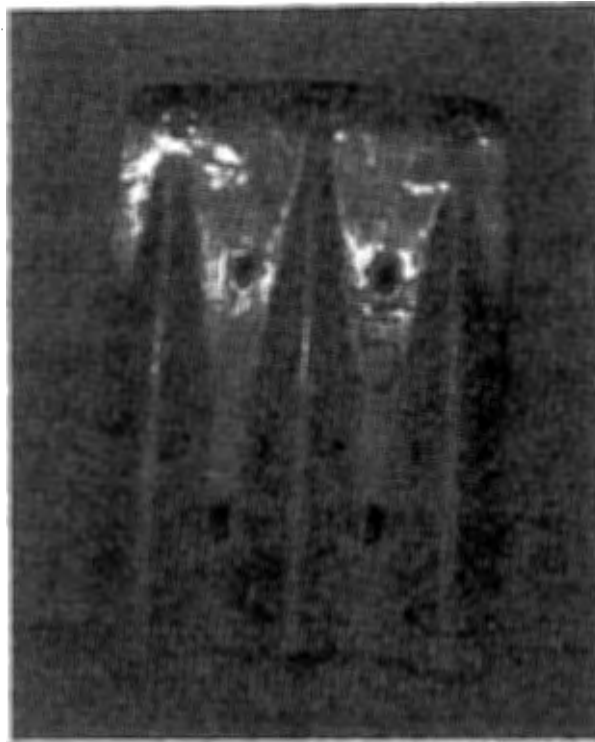


Figure 22. Full view of exterior damage, sample five.



Figure 23. Exterior damage to flat section, sample six.



Figure 24. Interior damage to flat section, sample six.

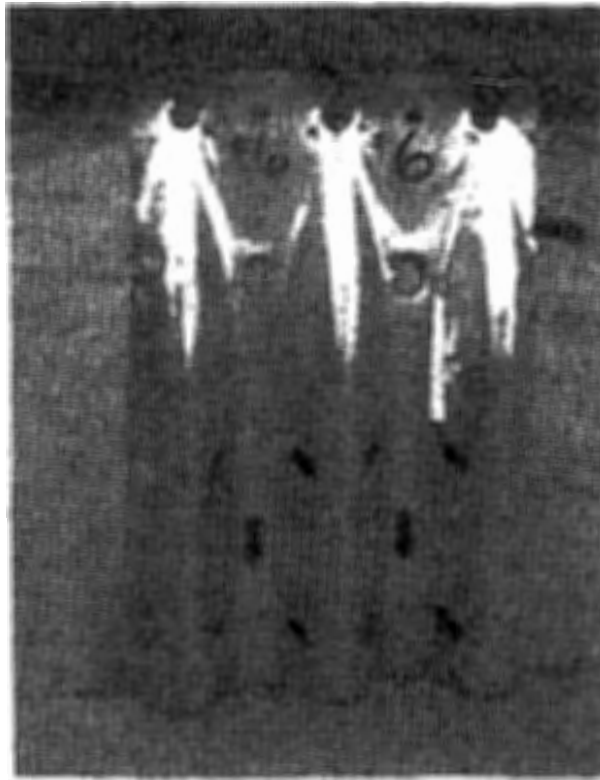


Figure 25. Full view of damaged connector, sample six.

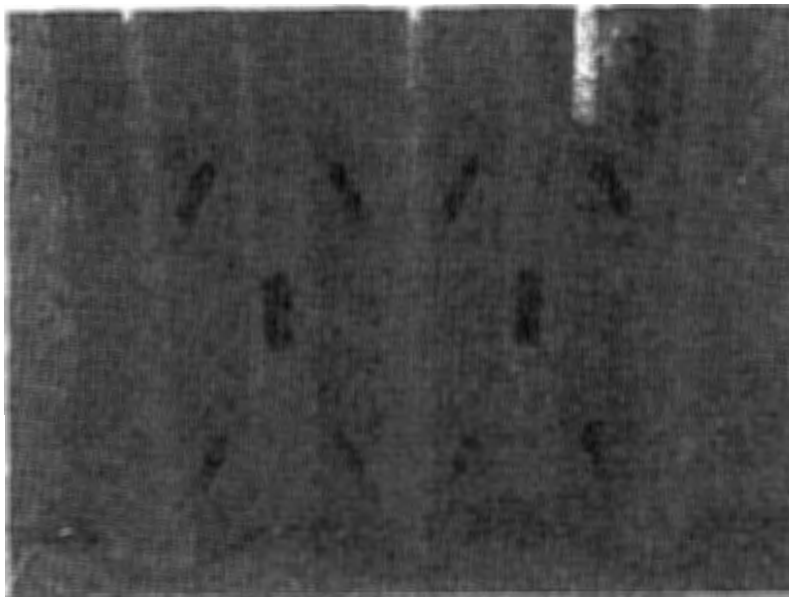


Figure 26. Damage at splice connection, sample six.

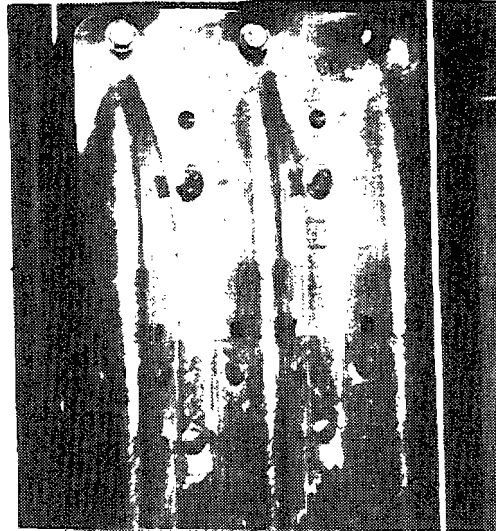


Figure 27. Terminal connector and test piece after test, sample eight.

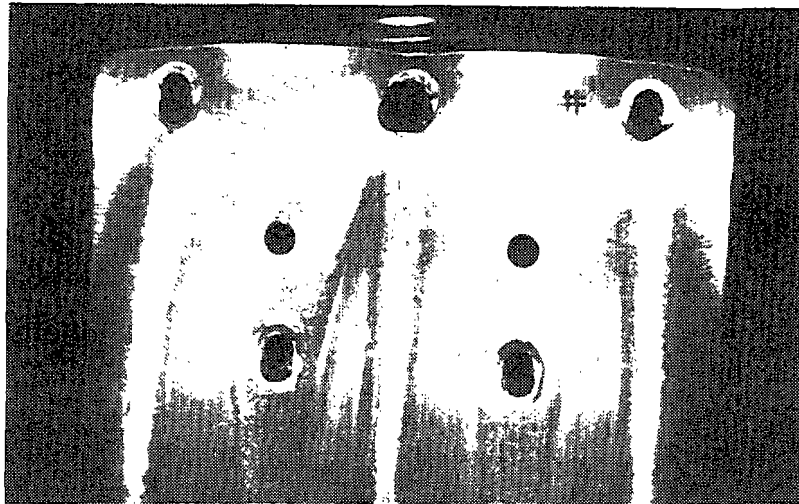


Figure 28. Exterior damage to flat section, sample eight.



Figure 29. Local buckling at edge of connector, sample eight.

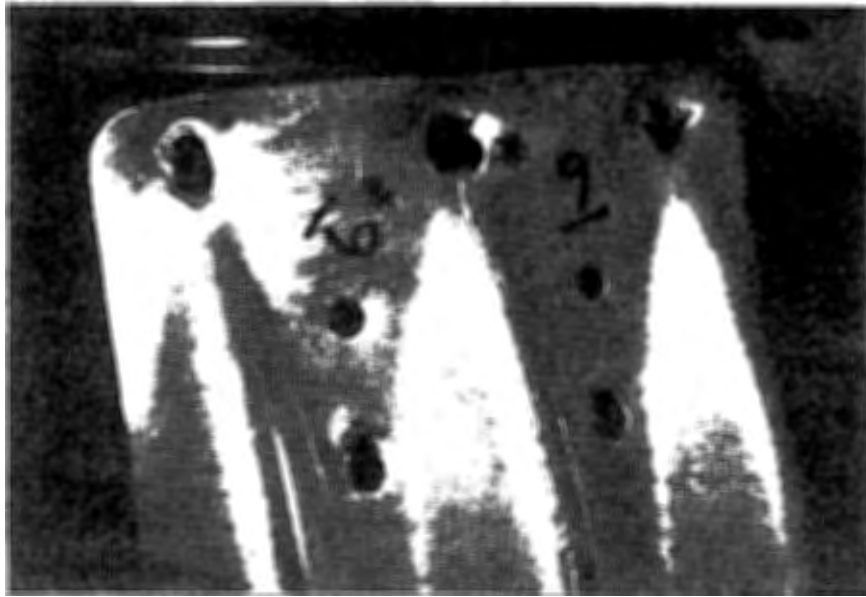


Figure 30. Exterior damage to flat section, sample nine.

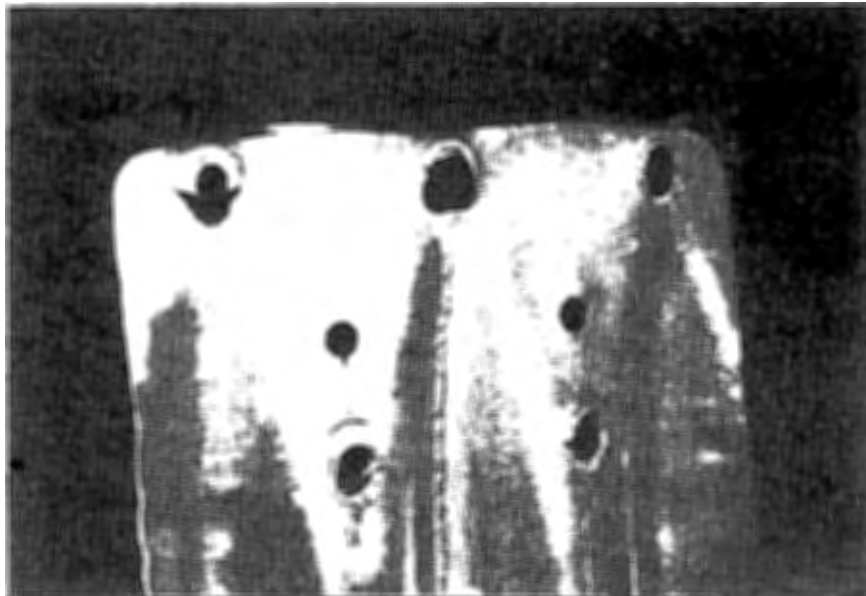


Figure 31. Interior damage to flat section, sample nine.



Figure 32. Terminal connector prior to testing.

Figure 33. Exterior damage at flat section, sample ten.

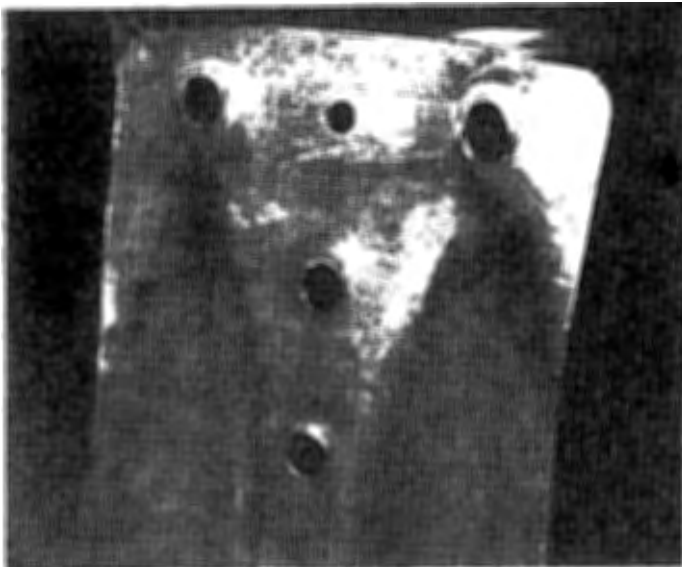
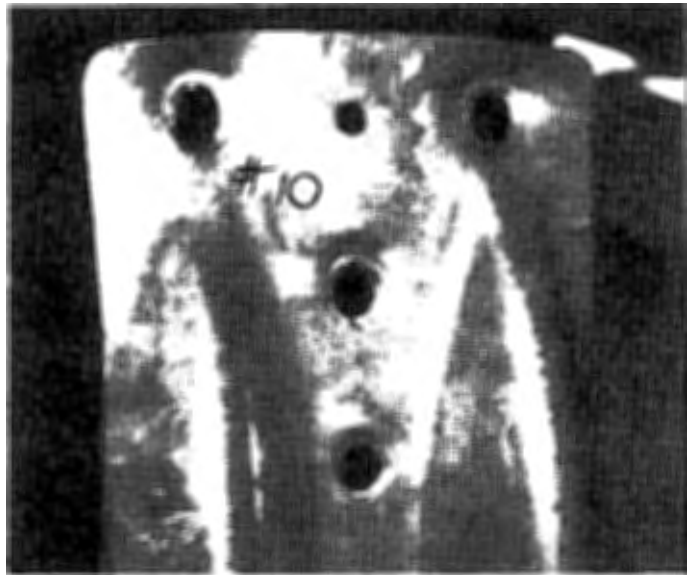


Figure 34. Interior damage of flat section, sample ten.



Figure 35. Interior view of terminal connector after test, sample eleven.

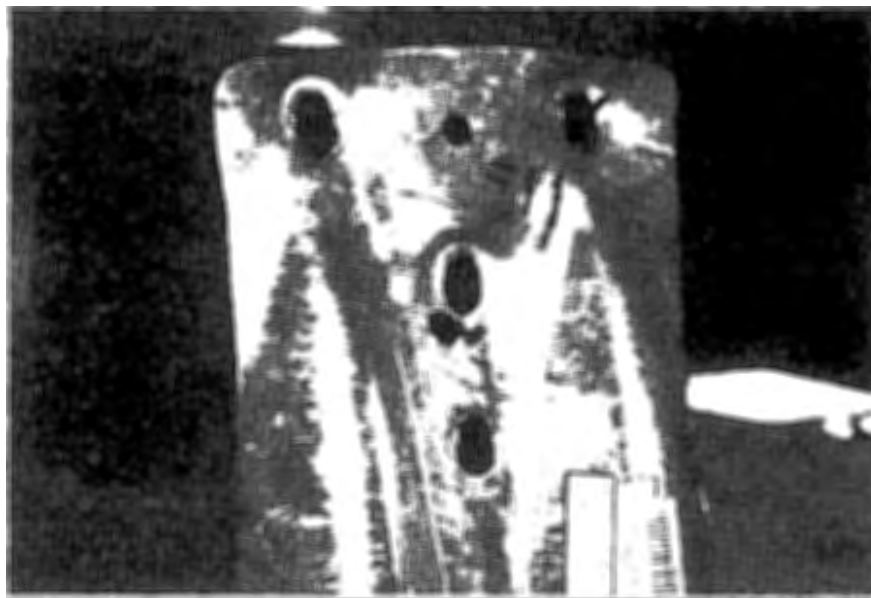


Figure 36. Exterior damage to flat section, sample eleven.

load direction (figure 36). Failure occurred at 65.9 kips (293.1 kN) and 66.4 kips (295.3 kN) for samples ten and eleven, respectively (table 1).

Sample twelve was a 12 gauge w-beam terminal connector with straight elongated slots at the splice end (figure 7). Failure was in bearing of the 7/8-in (22.2-mm) diameter bolts onto the flat section. Additionally, there was vertical tearing (parallel to the longitudinal axis and direction of the load) of each 1-in (25.4-mm) bolt hole on the top row of 1-in (25.4-mm) bolt holes. Buckling also occurred at the region between the upper row of 7/8-in (22.2m) bolts and the column of 7/8-in (22.2-mm) bolts in the flat section (figures 37 and 38). Deformation occurred at the splice connection but was limited to the interior slots on both the upper and lower rows (figure 39). The sample failed at 71.1 kips (316.2 kN) (table 1) which was somewhat larger than samples ten and eleven.

Samples thirteen, fourteen, and fifteen from manufacturer #2 were 10 gauge thrie-beam terminal connectors with angled slots at the splice end (figure 7). Failure was in bearing of the 7/8-in (22.2-mm) diameter bolts onto the flat section for all three specimens. Tearing of the steel at the upper right hand bolt hole occurred for all samples, particularly sample fourteen (figures 40, 41, and 42). There was virtually no structural damage at the splice ends on any of the specimens (figures 43, 44, and 45). There was local buckling at the top edge of the flat section near the upper three 7/8-in (22.2-mm) diameter bolts (figures 46, 47, and 48). Five 7/8-in (22.2-mm) diameter bolts were used in the flat portion of each terminal connector, and twelve 5/8-in (16-mm) mild steel button head bolts were used in the splice end of each connector. Unlike the other specimens, no bolts were included in the post mounting slots. Ultimate load capacities for samples thirteen, fourteen, and fifteen were 102.4 kips (455.5 kN), 99.3 kips (441.7 kN), and 101.8 kips (452.8 kN) respectively (table 1).

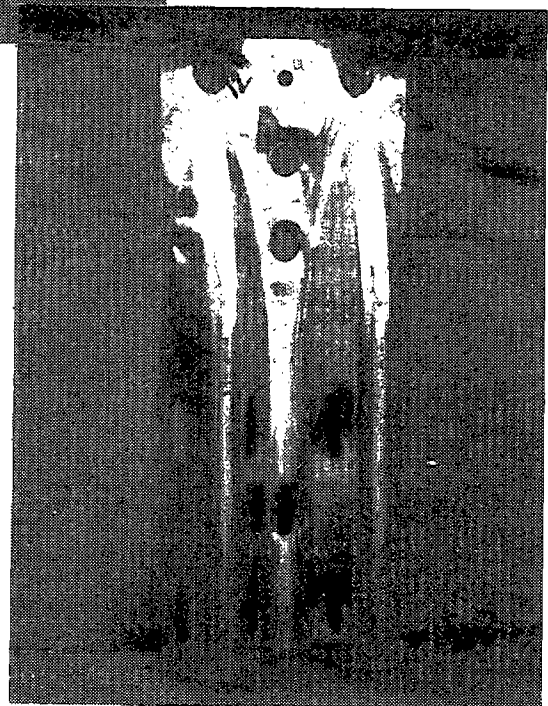


Figure 37. Exterior damage to flat section, sample twelve.



Figure 38. Interior damage to flat section, sample twelve.

Figure 39. Damage at splice end, sample twelve.



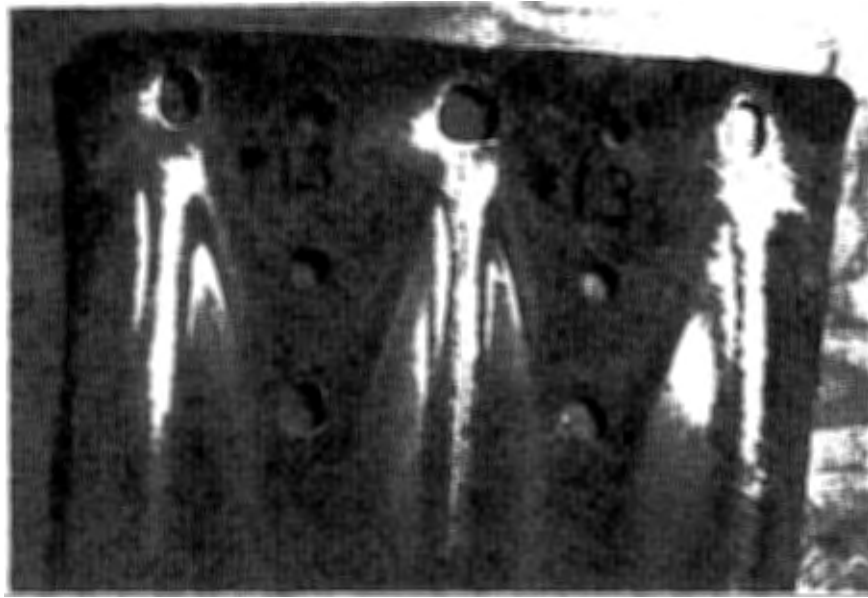


Figure 40. Damage at flat section, sample thirteen.

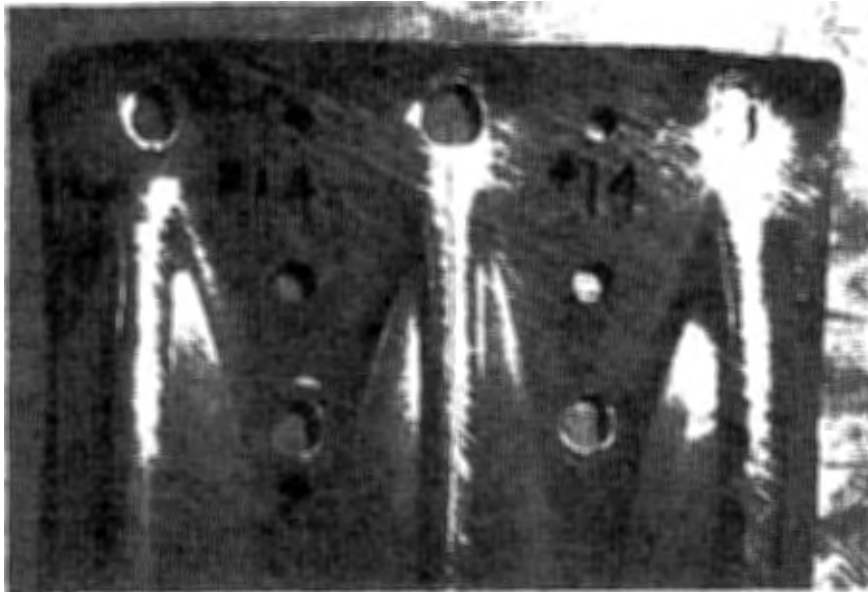


Figure 41. Damage at flat section, sample fourteen.

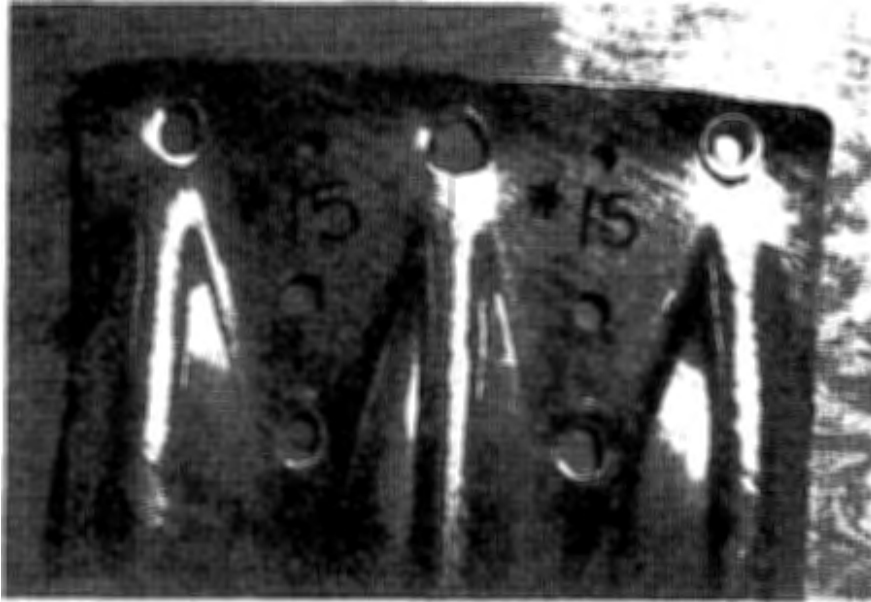


Figure 42. Damage at flat section, sample fifteen.

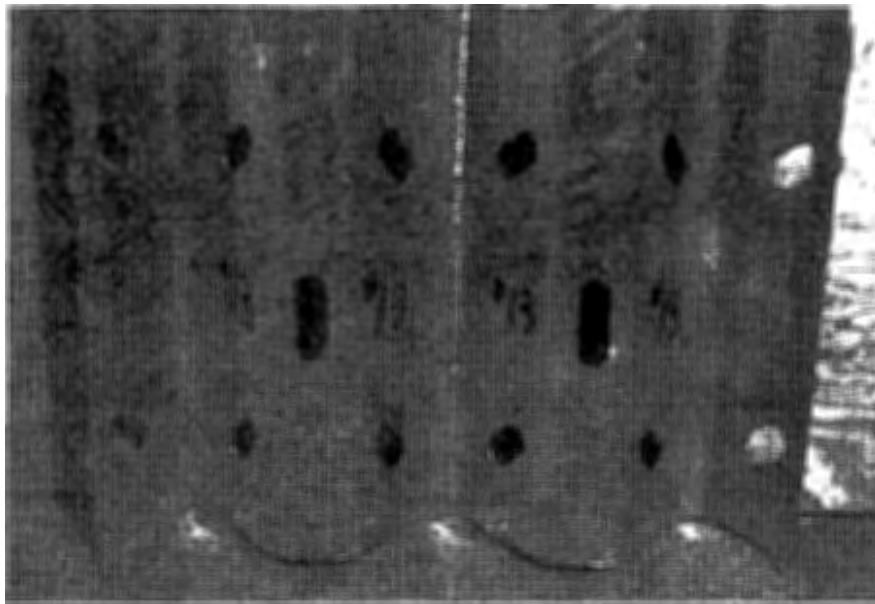


Figure 43. Damage at splice end, sample thirteen.

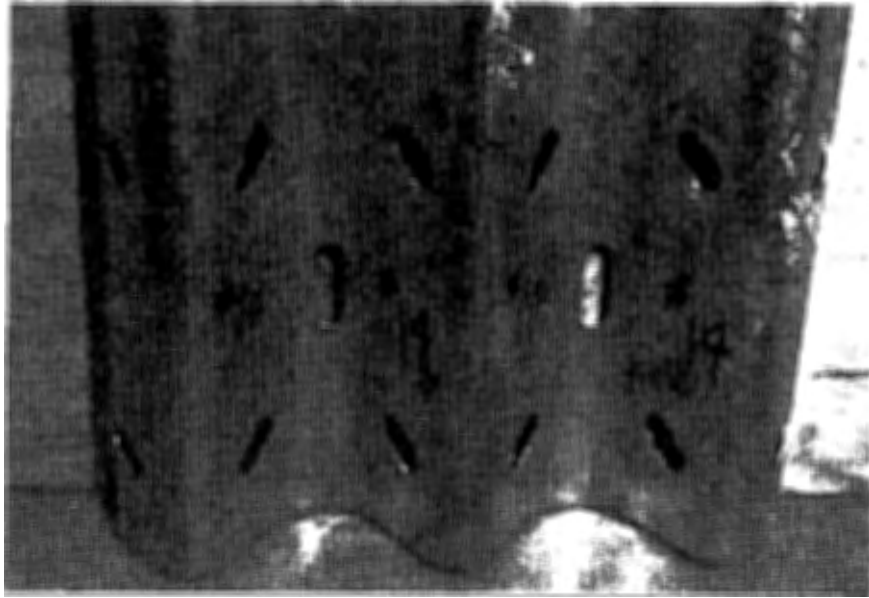


Figure 44. Damage at splice end, sample fourteen.

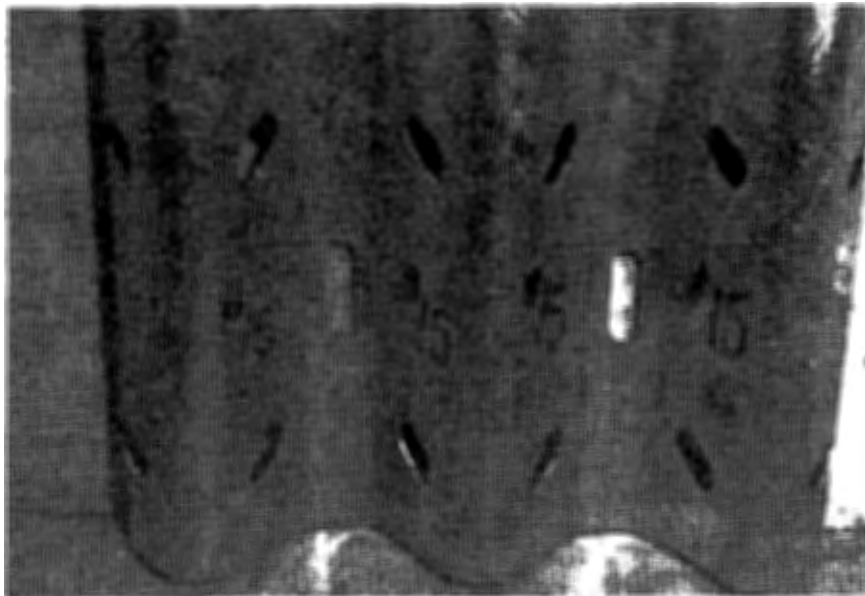


Figure 45. Damage at splice end, sample fifteen.



Figure 46. Local buckling of terminal connector, sample thirteen.

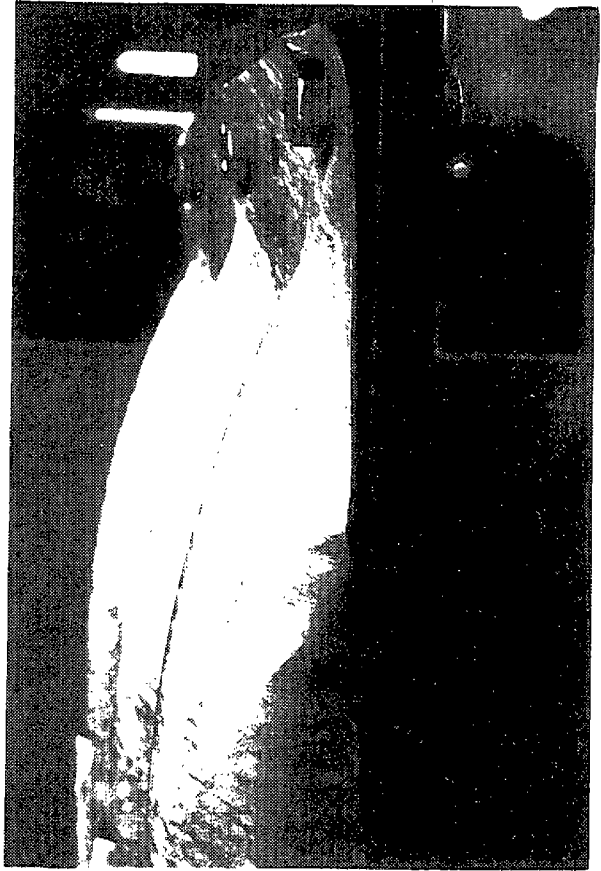


Figure 47. Local buckling of terminal connector, sample fourteen.

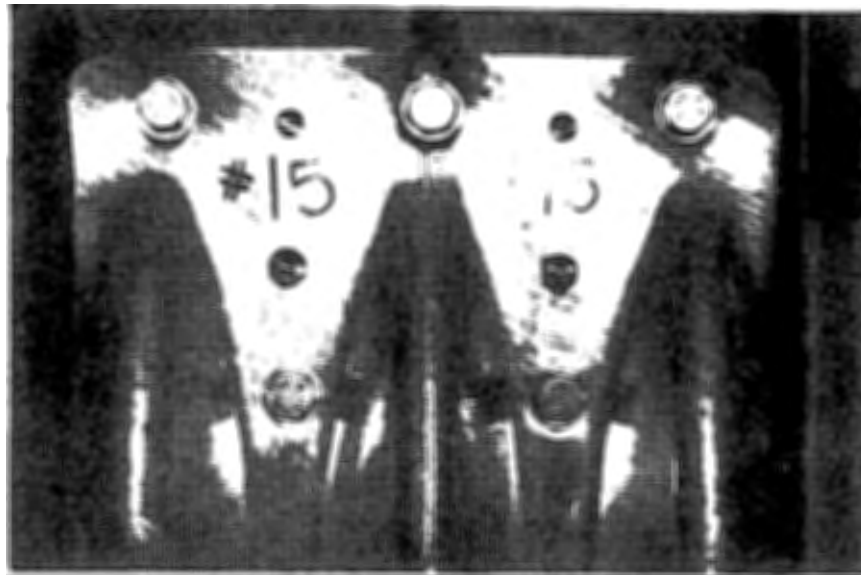


Figure 48. Local buckling of terminal connector, sample fifteen.

CHAPTER 4. CONCLUSIONS

Several variations of w-beam and thrie-beam terminal connectors were tested making it difficult to attain any real comparable conclusions about the axial capacity of angled splice slots versus straight slots. It can be concluded, however, that the splice connection did not affect the performance or static load capacity of any of the samples tested.

The graphs of samples one, five, six, eight, and nine revealed three distinct slopes. The steepest slope can be attributed to the elastic region of the material. The second slope exhibits bearing of the bolts into the flat section of the terminal connector. The third slope, leading to failure, exhibits plastic flow and tearing at the 1-in (25.4-mm) holes in the flat section of the terminal connector.

The graph of sample two in the appendix shows a sharp decrease in the load at approximately 80 kips (355.8 kN). One of the bolts at the splice connection slipped, resulting in a load decrease followed by an immediate recovery. The exact location of the slippage was unattainable. However, it can be attributed to the splice bolts because the bolts in the flat section were bearing against the terminal connector at the beginning of the test.

As stated previously in the body of the report, many of the graphs start at a value other than zero for both the ordinate and the abscissa. The initial location of the ram (transient) head is a predetermined value that was input into the software. Any displacement of the ram head after initial input is relative to that initial value and is thus reflected on the graphs. The test article in each test was loaded to a maximum of 6 kips (27 kN) to remove any slack that might have existed in the system.

LOAD vs. DISPLACEMENT OF RAM HEAD SAMPLE 1

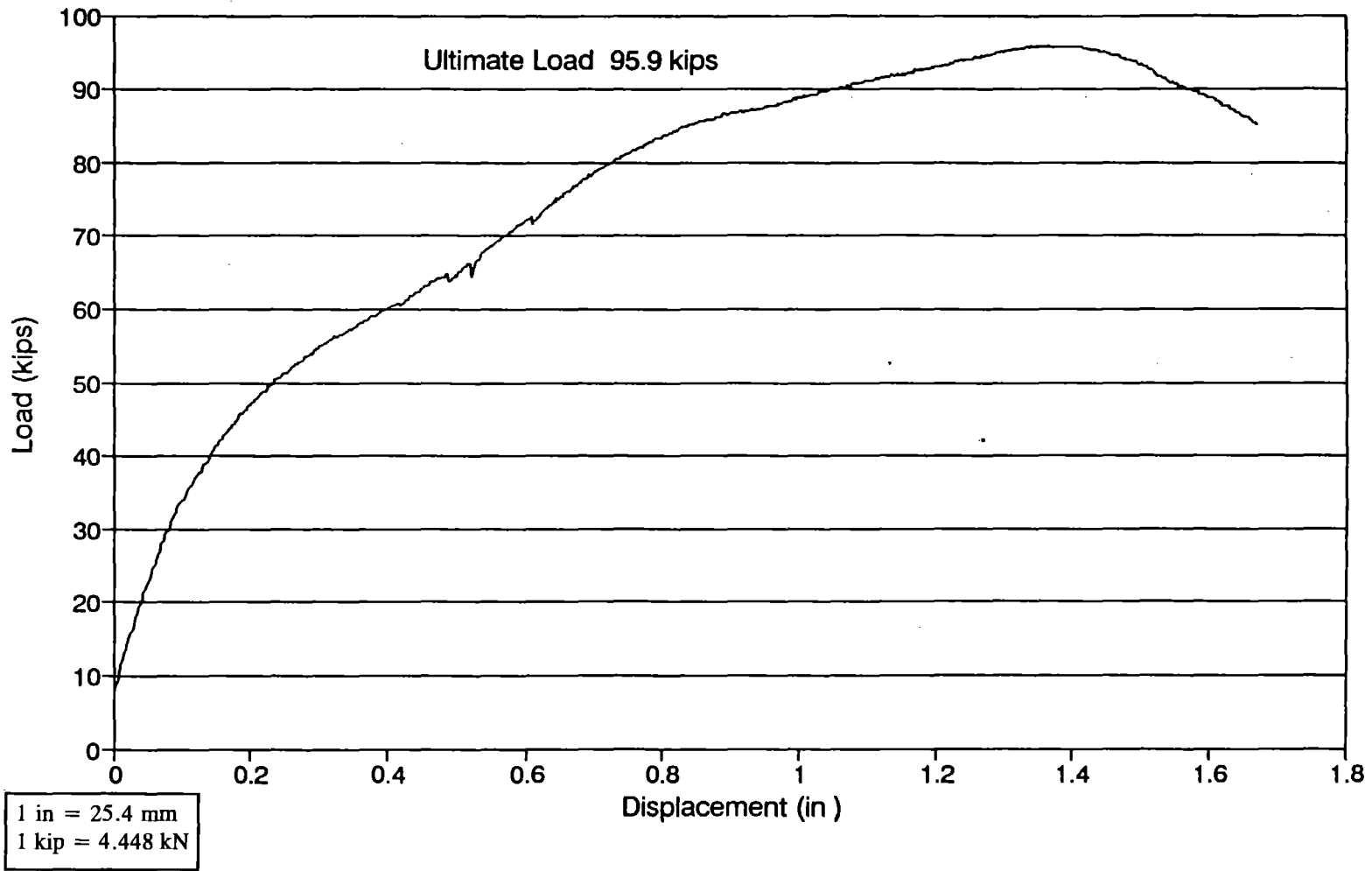


Figure 49. Load vs. displacement graph, sample one.

LOAD vs. DISPLACEMENT OF RAM HEAD SAMPLE 2

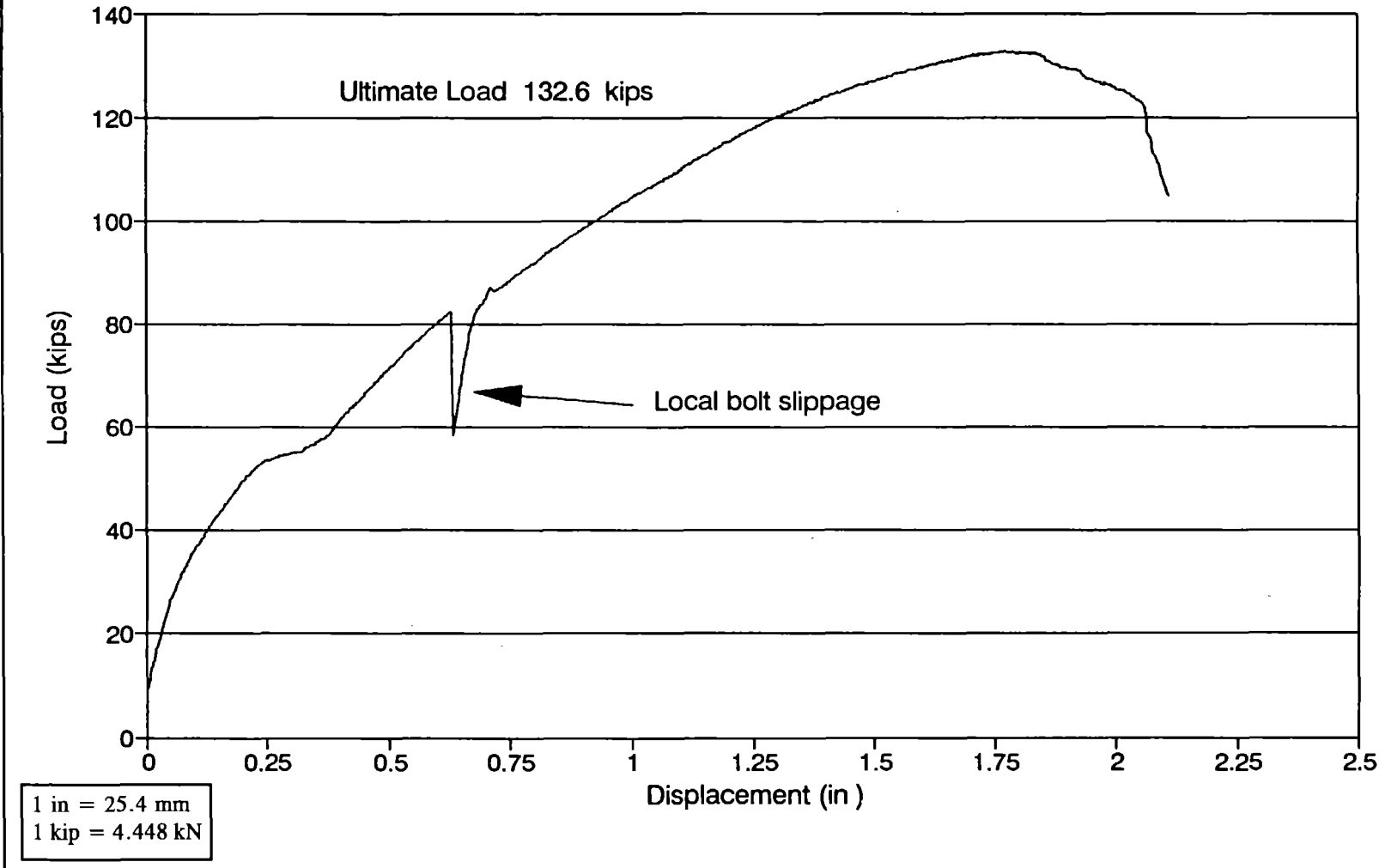
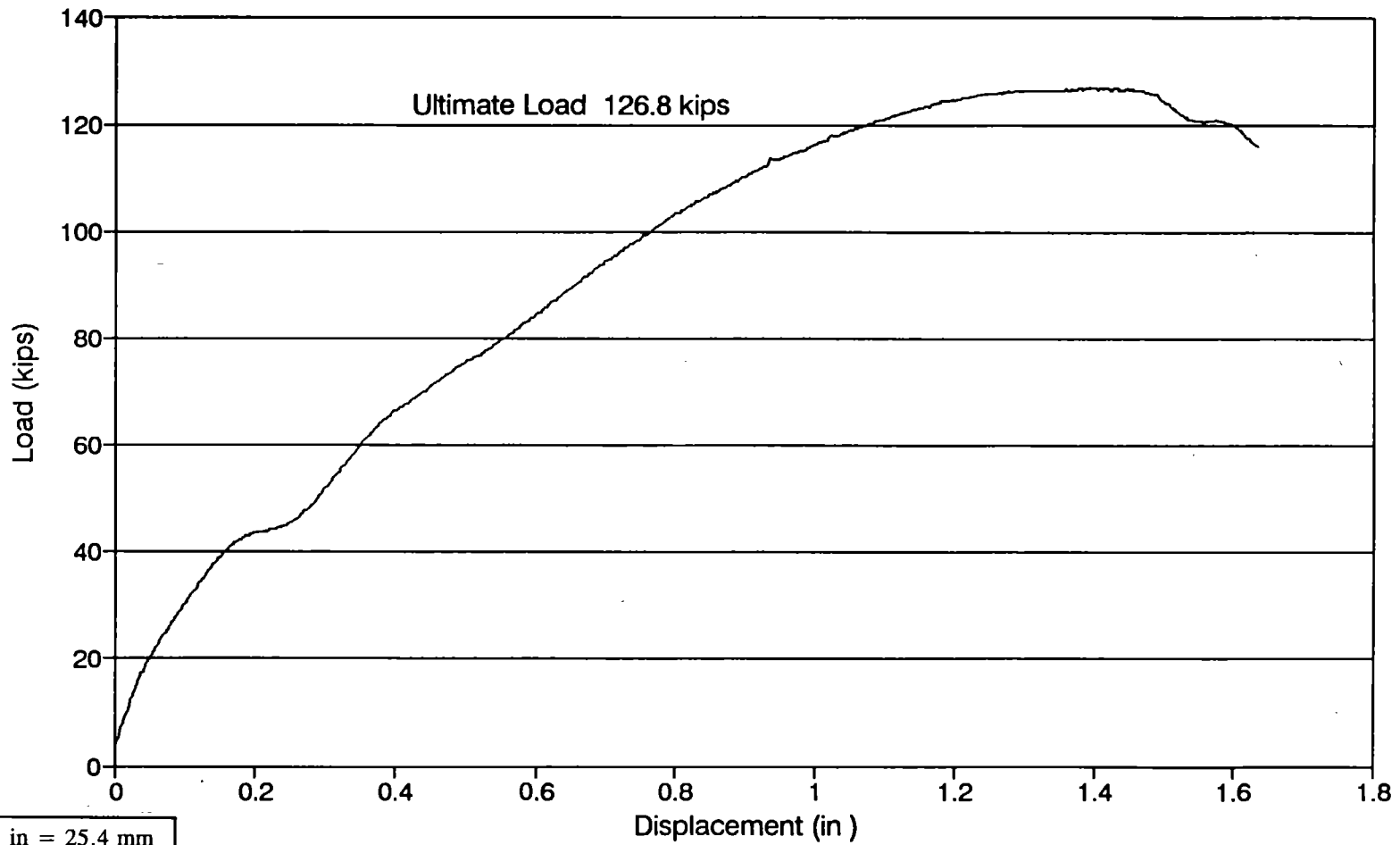


Figure 50. Load vs. displacement graph, sample two.

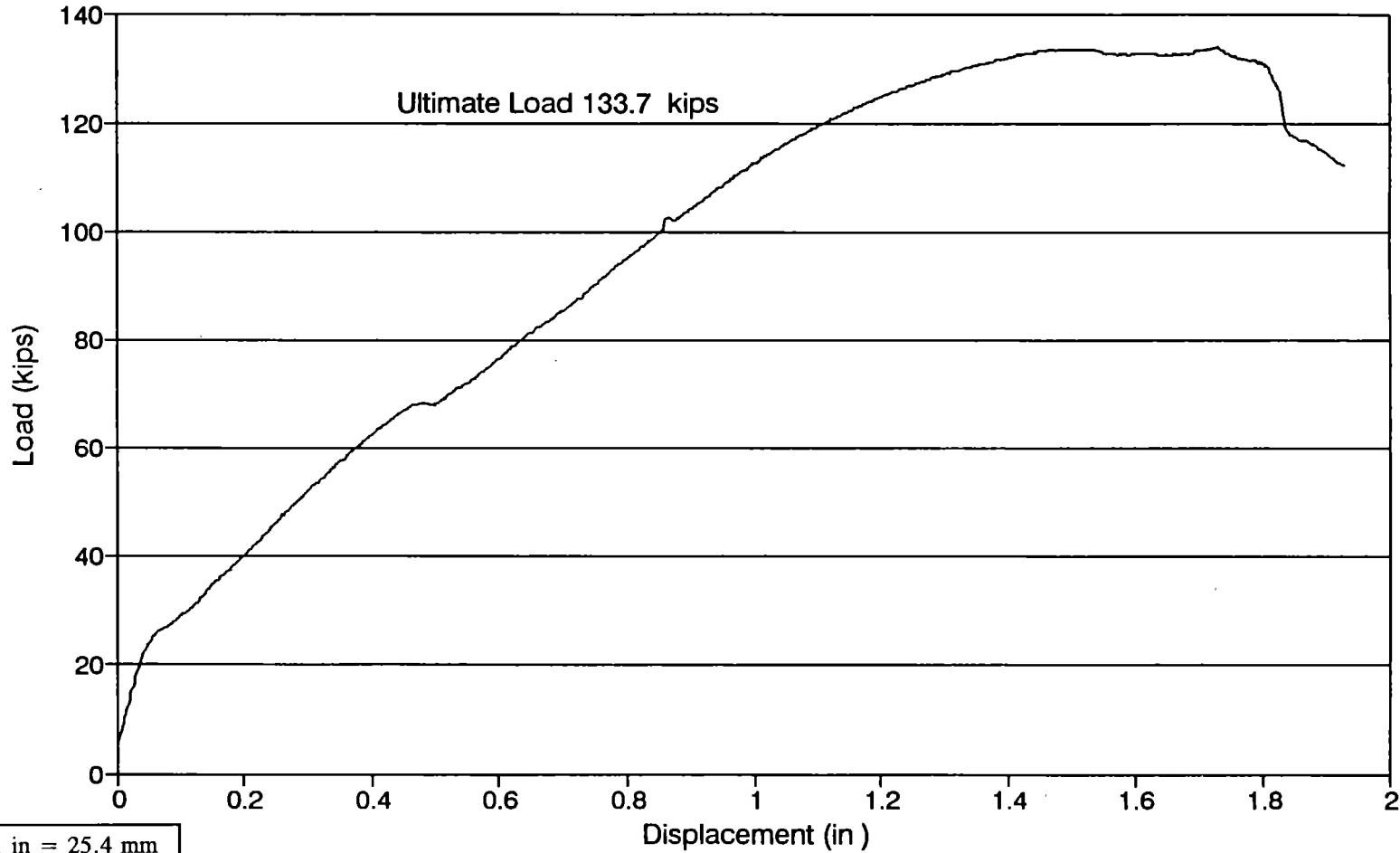
LOAD vs. DISPLACEMENT OF RAM HEAD SAMPLE 3



1 in = 25.4 mm
1 kip = 4.448 kN

Figure 51. Load vs. displacement graph, sample three.

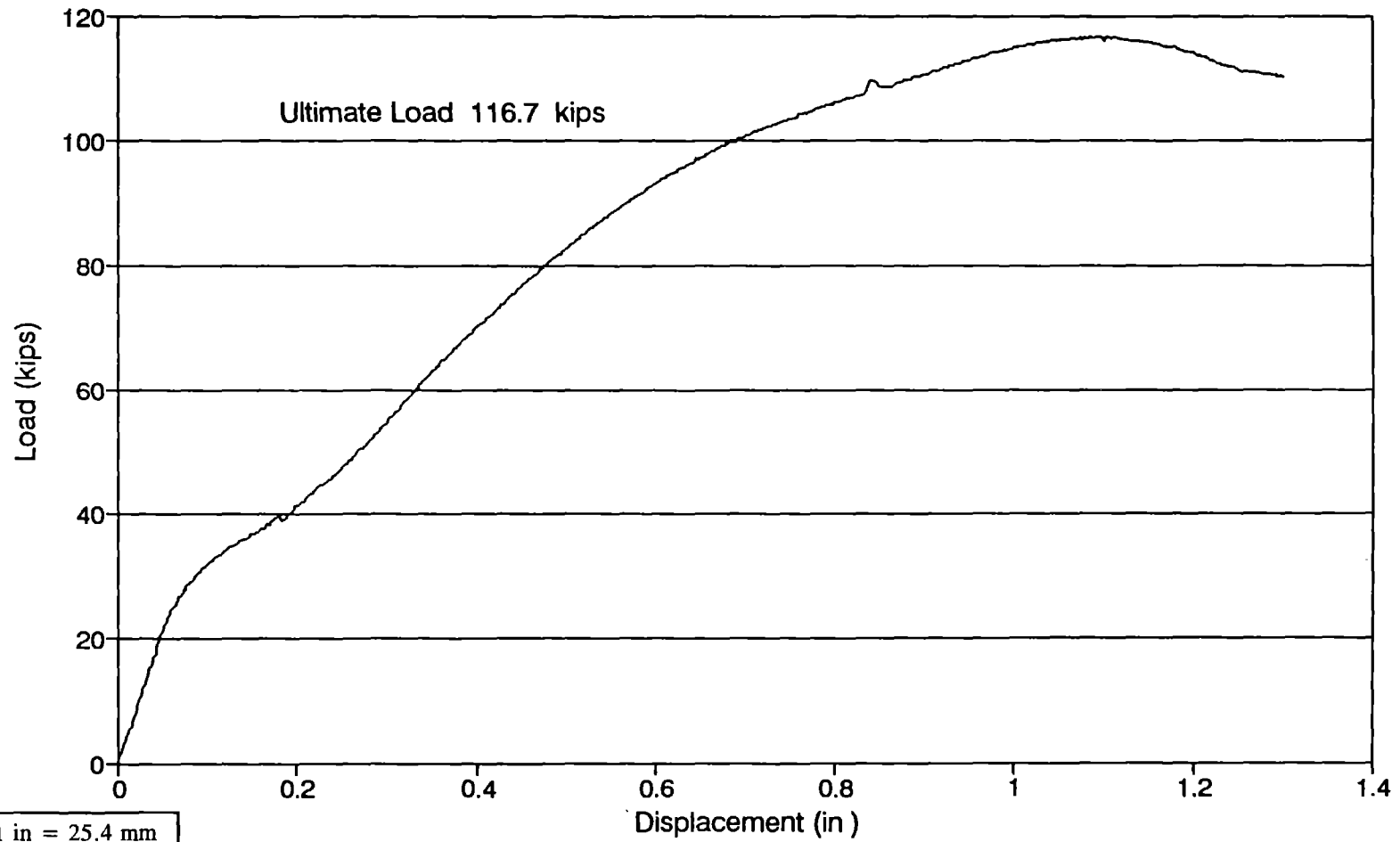
LOAD vs. DISPLACEMENT OF RAM HEAD SAMPLE 4



1 in = 25.4 mm
1 kip = 4.448 kN

Figure 52. Load vs. displacement graph, sample four.

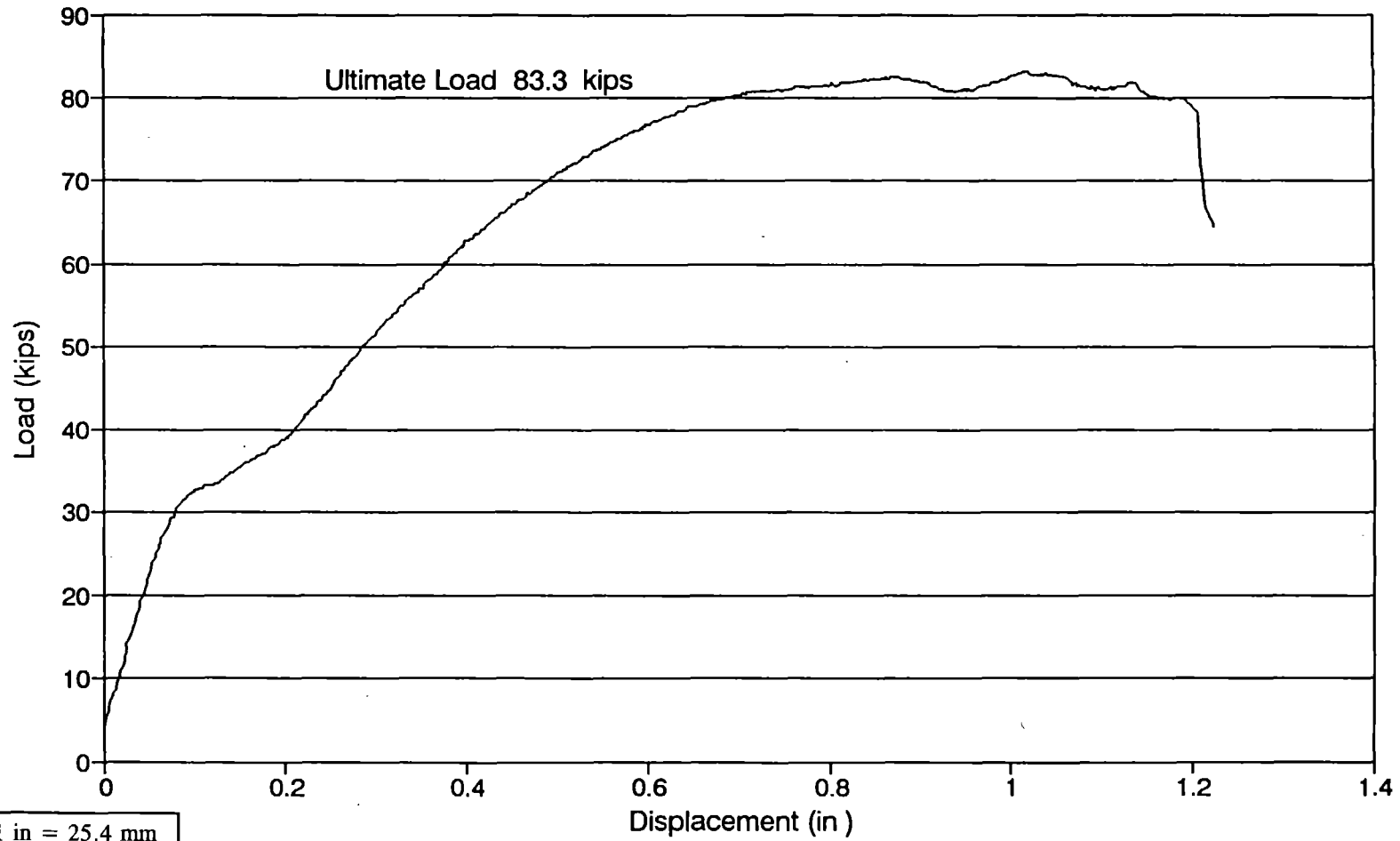
LOAD vs. DISPLACEMENT OF RAM HEAD SAMPLE 5



1 in = 25.4 mm
1 kip = 4.448 kN

Figure 53. Load vs. displacement graph, sample five.

LOAD vs. DISPLACEMENT OF RAM HEAD SAMPLE 6



1 in = 25.4 mm
1 kip = 4.448 kN

Figure 54. Load vs. displacement graph, sample six.

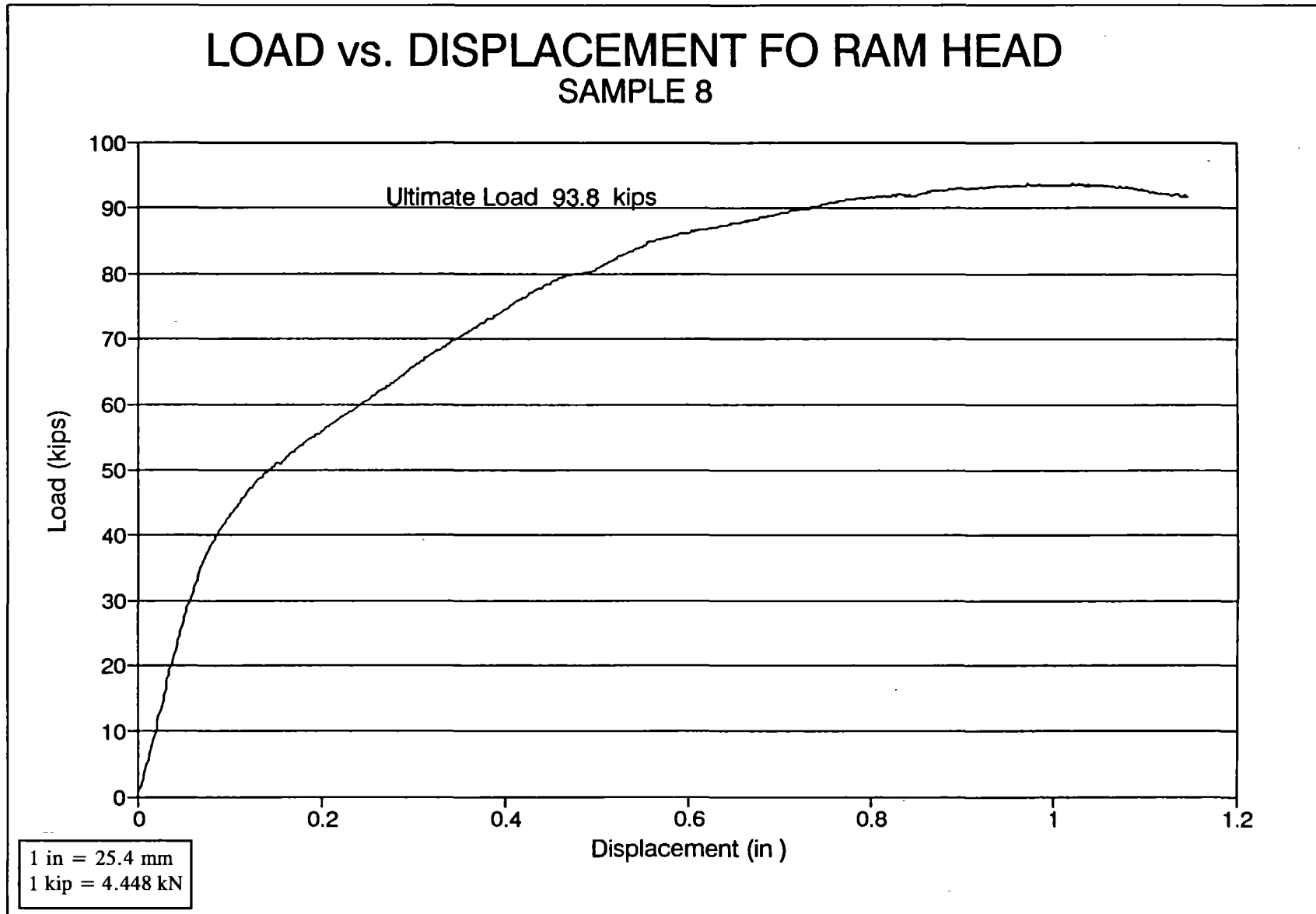
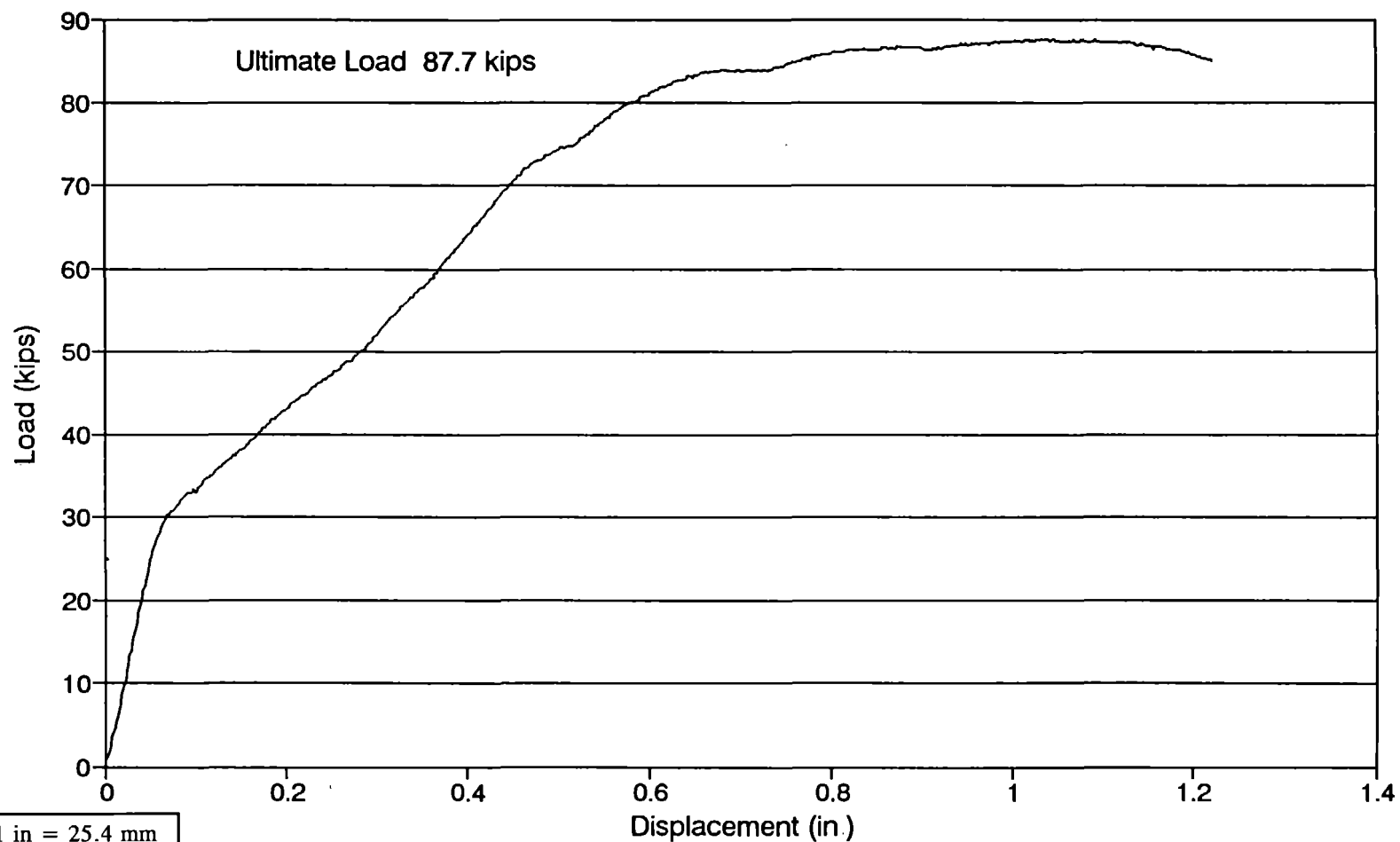


Figure 55. Load vs. displacement graph, sample eight.

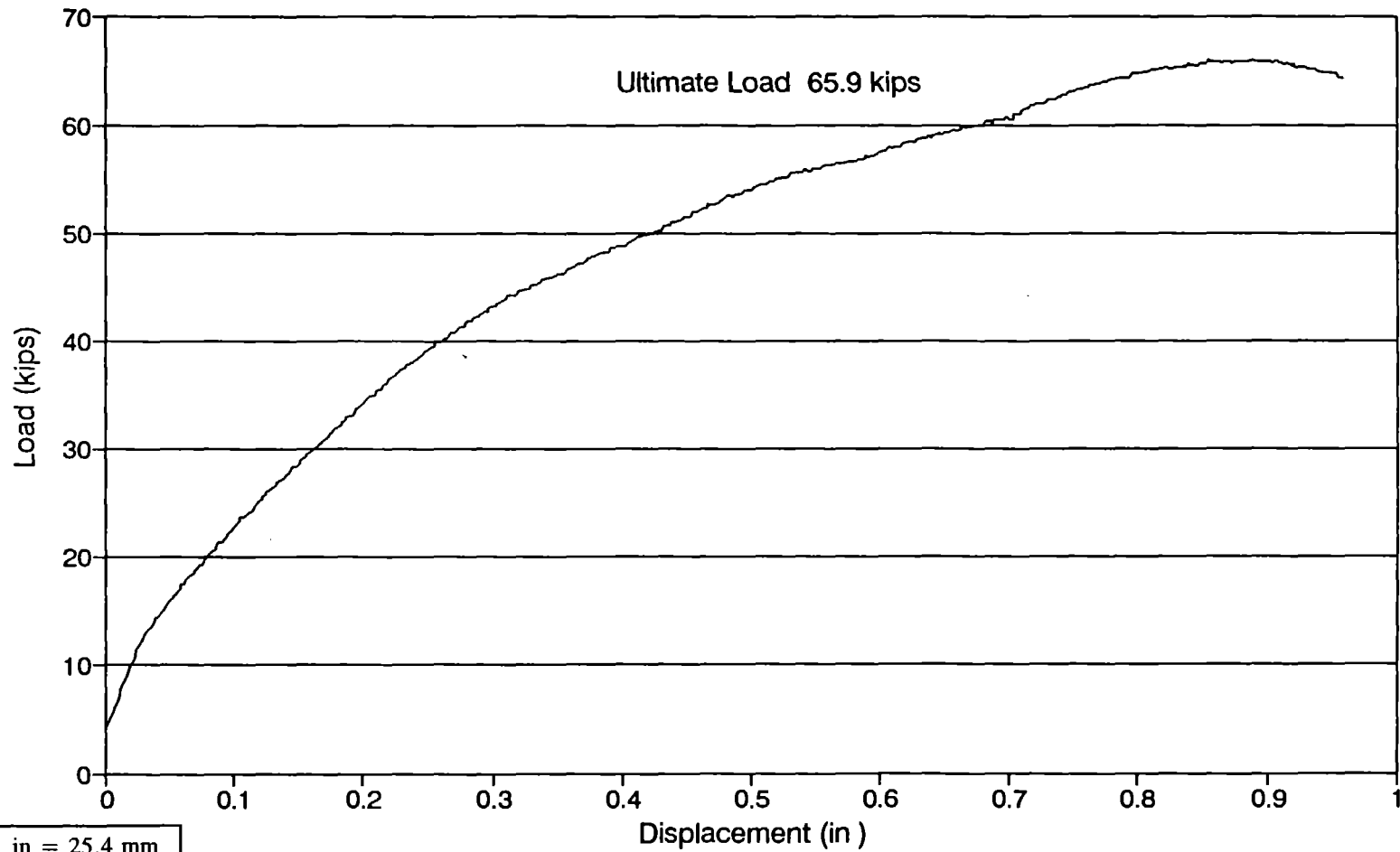
LOAD vs. DISPLACEMENT OF RAM HEAD SAMPLE 9



1 in = 25.4 mm
1 kip = 4.448 kN

Figure 56. Load vs. displacement graph, sample nine.

LOAD vs. DISPLACEMENT OF RAM HEAD SAMPLE 10



1 in = 25.4 mm
1 kip = 4.448 kN

Figure 57. Load vs. displacement graph, sample ten.

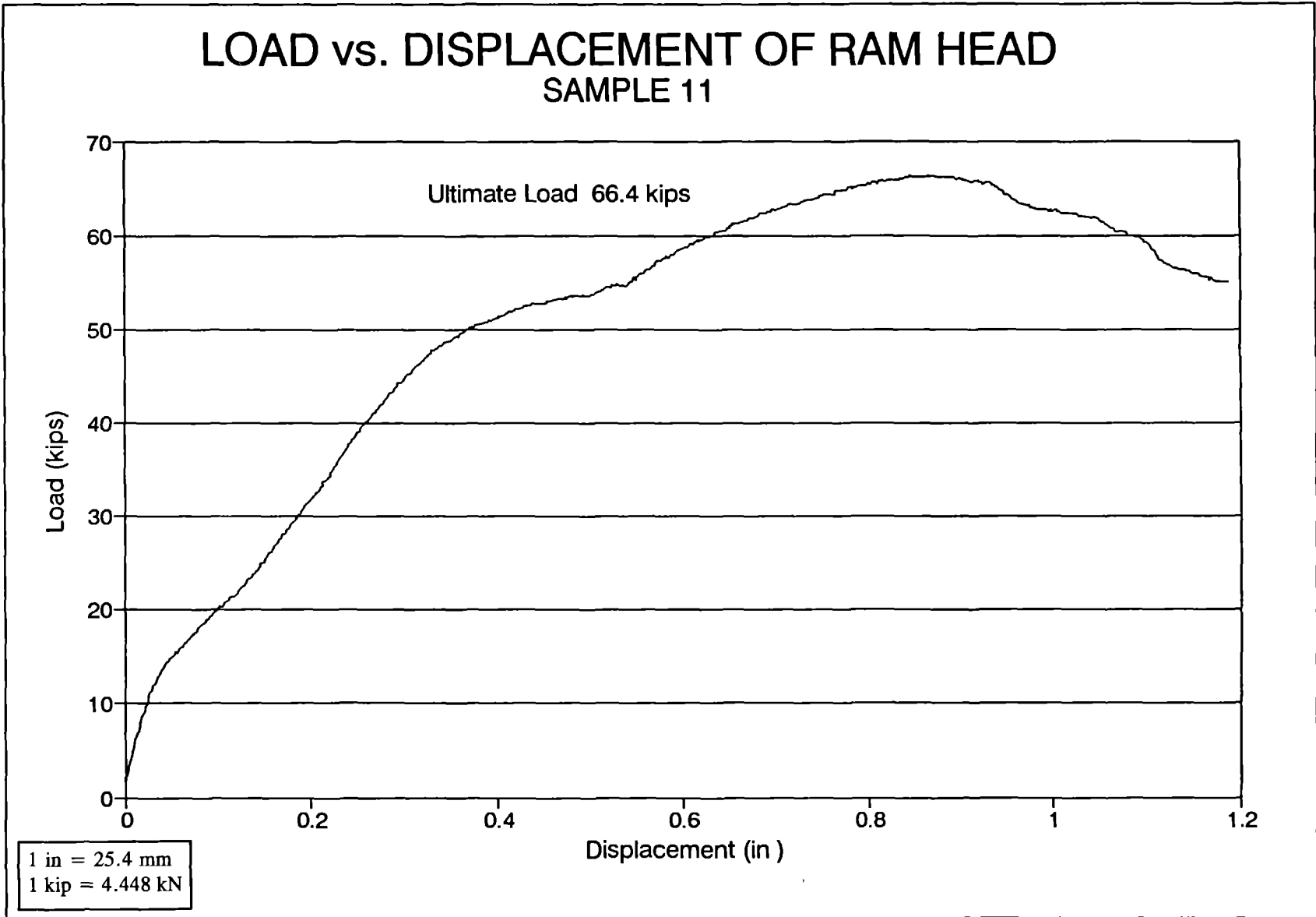
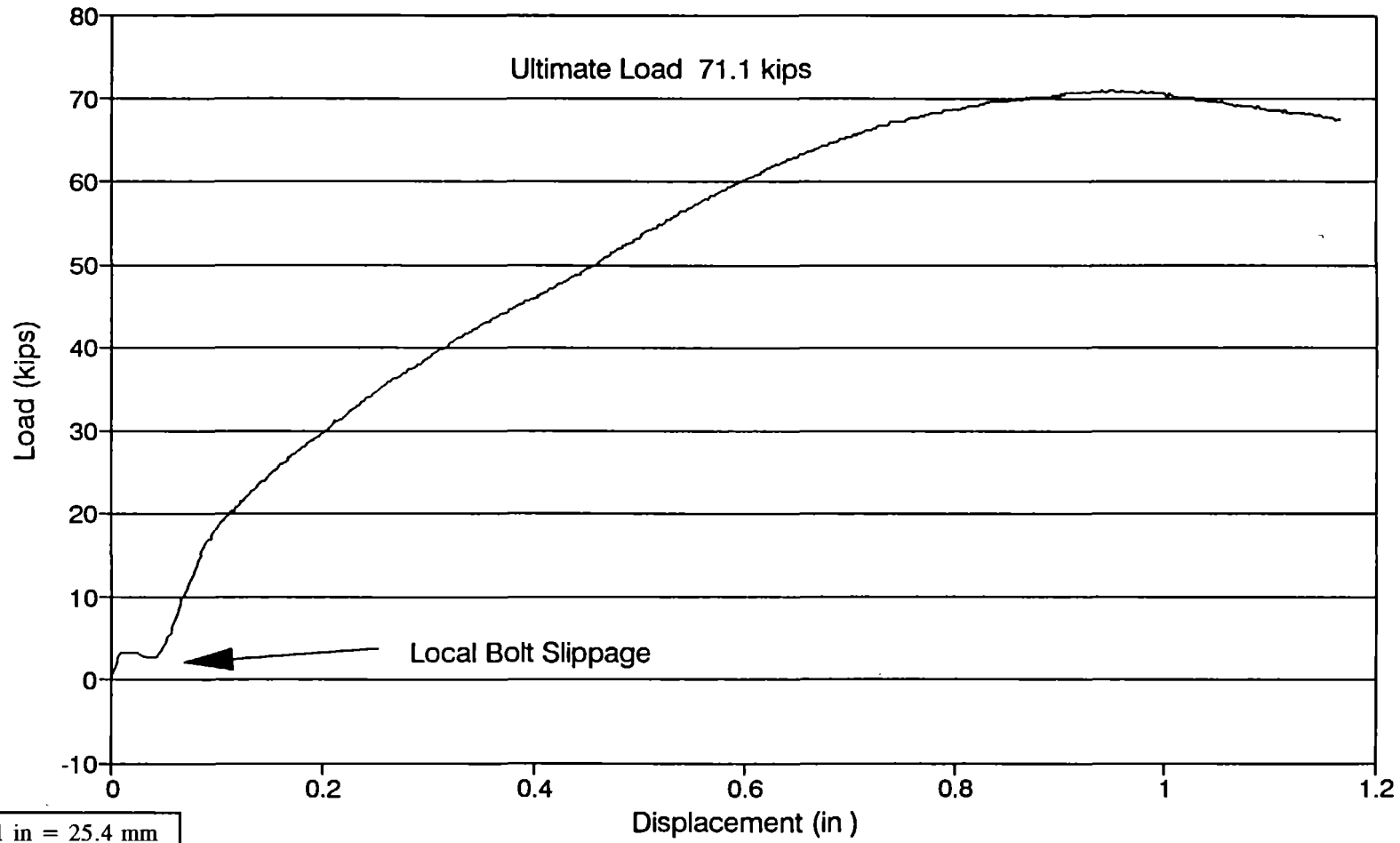


Figure 58. Load vs. displacement graph, sample eleven.

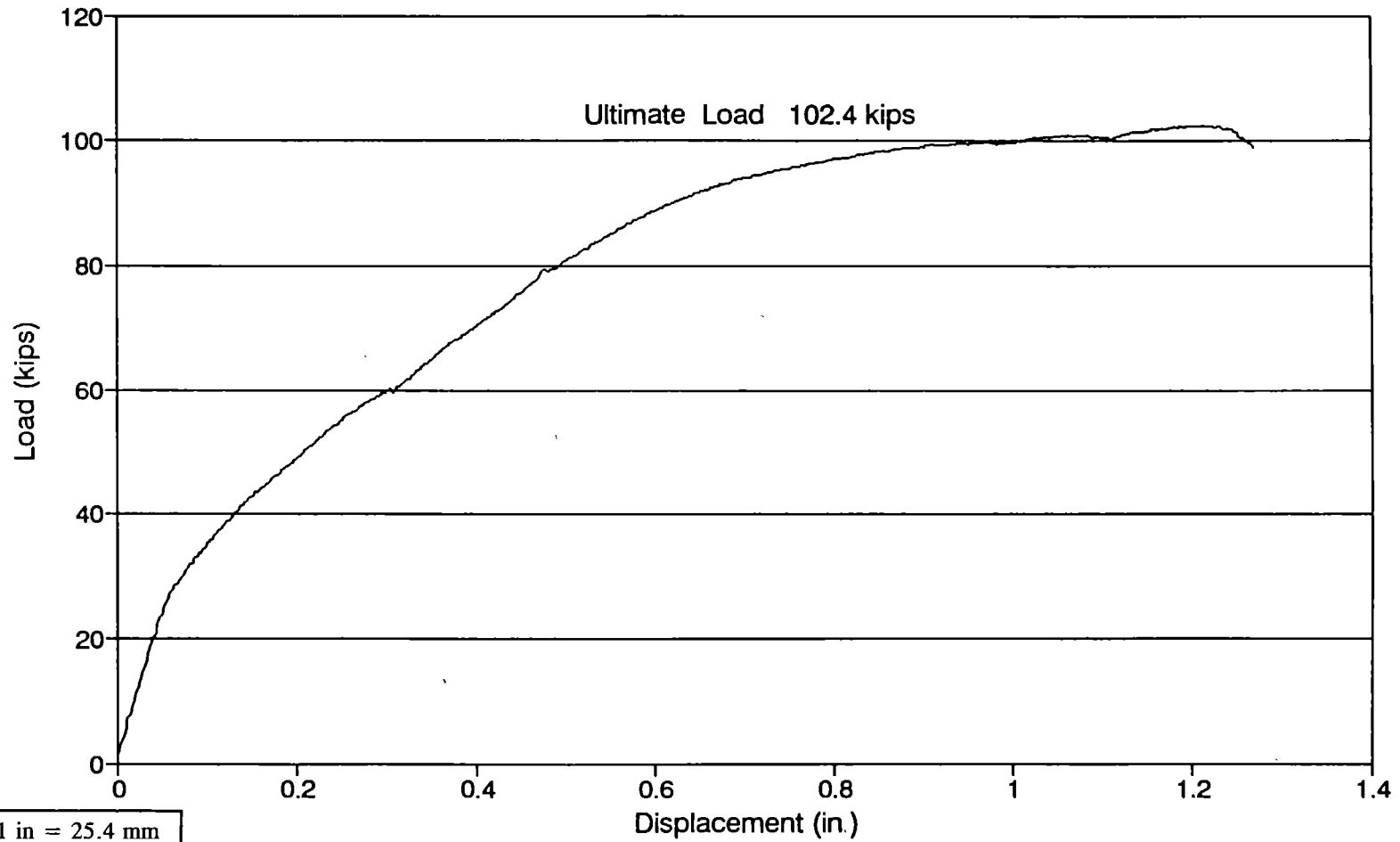
LOAD vs. DISPLACEMENT OF RAM HEAD SAMPLE 12



1 in = 25.4 mm
1 kip = 4.448 kN

Figure 59. Load vs. displacement graph, sample twelve.

LOAD vs. DISPLACEMENT OF RAM HEAD SAMPLE 13



1 in = 25.4 mm
1 kip = 4.448 kN

Figure 60. Load vs. displacement graph, sample thirteen.

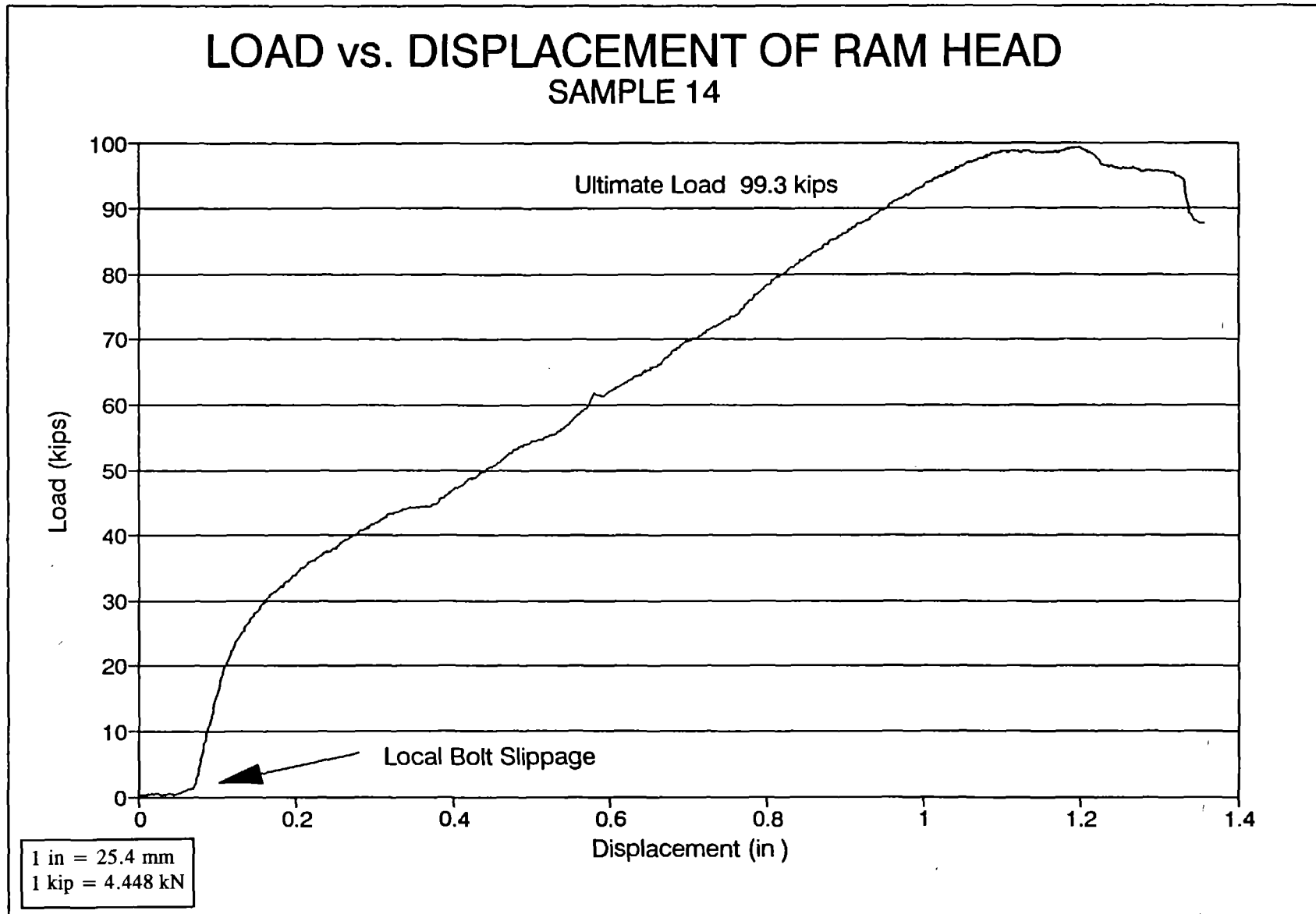


Figure 61. Load vs. displacement graph, sample fourteen.

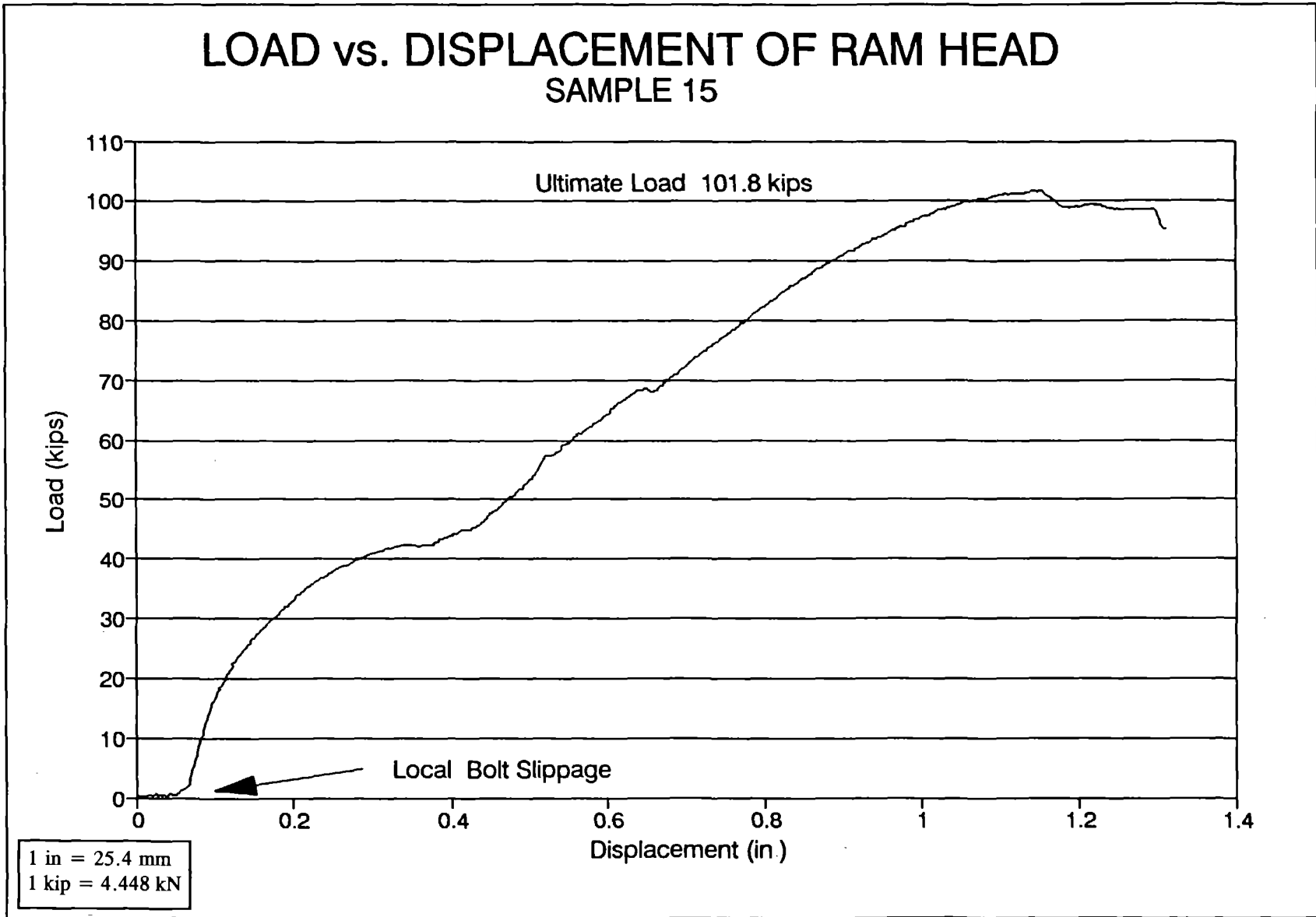


Figure 62. Load vs. displacement graph, sample fifteen.

